이 학 박 사 학 위 논 문

Slit guidance ligand 3가 β-catenin 억제에 의한 연골내골화 기전 연구

Slit guidance ligand 3 regulates endochondral ossification by β-catenin suppression in chondrocytes

울 산 대 학 교 대 학 원

의 학 과

최 영 진

Doctor of Philosophy

Slit guidance ligand 3 regulates endochondral ossification by β-catenin suppression in chondrocytes

The Graduate School

of the University of Ulsan

Department of Medicine

Choi, Young-Jin

Slit guidance ligand 3 regulates endochondral ossification by β-catenin suppression in chondrocytes

Supervisor : Jung-Min Koh

A Dissertation

Submitted to
the Graduate School of the University of Ulsan
In partial Fulfillment of the Requirements
for the Degree of

Doctor of Philosophy

By

Choi, Young-Jin

Department of Medicine
Ulsan, South Korea

December 2018

Slit guidance ligand 3 regulates endochondral ossification by β-catenin suppression in chondrocytes

This certifies that the dissertation
of Choi Young-Jin is approved.

이 승 훈

Committee Chair M.D., Ph.D.

김 정 은

Committee Member Ph.D.

김 경 곤

Committee Member Ph.D.

유 현 주

Committee Member Ph.D.

고 정 민

Committee Member M.D., Ph.D.

Department of Medicine

Ulsan, South Korea

December 2018

Abstract

Slit guidance ligand 3 (Slit3) has an osteoprotective role by stimulating bone formation and suppressing bone resorption. Additionally, it is found that global *Slit3* KO mice had smaller long bone. Skeletal staining showed a short mineralized length in newborn KO mice and a wide hypertrophic chondrocyte area in KO embryos, suggesting delayed chondrocyte maturation. Recombinant Slit3 did not cause any change in the proliferation of ATDC5 cells, but induced the expression of genes associated with chondrocyte differentiation, including *Hif1a*, *Acan* (aggrecan), *Col2a1*, *Sox9*, *Col10a1*, *Vegf*, and *Mmp13*. Slit3 suppressed β-catenin activity in ATDC5 cells, and activation of Wnt/β-catenin signaling with lithium chloride attenuated the Slit3-induced expression of differentiation markers. Among the four Roundabout (Robo) isoforms, ATDC5 cells expressed only Robo2, and *Robo2* knockdown with siRNA inhibited the expression of chondrocyte differentiation markers in response to stimulation with Slit3. Similarly, *Robo2* KO mice showed delayed hypertrophic differentiation of the long bone. Taken together, these data indicate that Slit3 and

Robo2 promote chondrocyte maturation via the inhibition of β-catenin signaling.

Keywords: Slit3, endochondral ossification, chondrocytes, Robo2, β-catenin

Contents

List of Figures

1. Introduction

The vertebrate skeleton, which consists of cartilage and bone, is the product of three distinct embryonic lines of cells. The craniofacial skeleton derives from skull nerve crest cells, the axial skeleton is derived from paraxial mesoderm (somites), and the limb skeleton derives from lateral plate mesodermal cells [1]. Bone development involves two types of ossification, endochondral and intramembranous ossification [2][3][4]. Craniofacial bone is formed directly from the condensation of mesenchymal cells without the formation of cartilaginous intermediates, a process known as intramembranous ossification. By contrast, endochondral ossification is a key process for long bone growth in the developing embryo. During endochondral ossification, mesenchymal stem cells (MSCs) first condense, which is followed by chondrocyte differentiation. Perichondrium is formed around the differentiated chondrocytes. The chondrocytes then proliferate and undergo progressive maturation through pre-hypertrophy and hypertrophy. The centrally localized chondrocytes proliferate actively before they exit the cell cycle and differentiate into hypertrophic chondrocytes.

Sequential differentiation of cartilage cells establishes the unique cell structure of the growth plate. At the end of the epiphyseal growth plate, the hypertrophic chondrocytes mineralize their own matrix. Multiple stages of differentiation produces a thin mesenchymal cell layer surrounding the cartilage matrix called the periosteum, which allows invading blood vessels and osteoclasts to migrate into the hypertrophic chondrocyte. While osteoclasts degrade substrates of the hypertrophic chondrocyte area, osteoblasts accumulate minerals. The cartilage matrix destroyed by osteoclasts forms a scaffold onto which osteoblasts deposit minerals (Fig. 1) [4]. Endochondral ossification is not only an essential process in the development and growth of long bones, but also occurs during the repair of broken bones [5].

These sequential steps are tightly regulated by multiple signaling pathways, including Indian hedgehog (Ihh), transforming growth factor (TGF)-β, parathyroid hormone (PTH), bone morphogenetic protein (BMP), and Wnt/β-catenin signaling [2][6][7][8][9][10]. Ihh is an important signaling pathway during endochondral ossification, and it is expressed in pre-hypertrophic and hypertrophic chondrocytes

[11]. TGF-β plays a central role in chondrocyte maturation and endochondral ossification. Activation of TGF-β by matrix metalloprotease 13 (MMP13) occurs in proliferating and hypertrophic chondrocytes [12]. PTH and PTH-related protein (PTHrP) directly regulate the pace and synchrony of chondrocyte differentiation [13]. BMP and Ihh signaling are required to maintain normal proliferation of chondrocytes. BMP signaling also delays hypertrophic differentiation in the limb [14].

Among these pathways, Wnt/β-catenin controls multiple steps of skeletal development. It regulates not only osteoblast differentiation but also chondrogenesis [15]. β-catenin enhances differentiation of MSCs into osteoblasts, but suppresses their differentiation into chondrocytes [16][17]. During early bone development, β-catenin is therefore suppressed to enhance chondrocyte differentiation, and is activated in later stages to enhance osteoblast differentiation. Conditional inactivation of the gene encoding β-catenin (*Ctnnb1*) during early skeletal development causes ectopic cartilage formation [16][17]. A low level of Wnt signaling therefore initially promotes differentiation into chondrocytes, and expression of Runt-related transcription factor

(Runx)2 is induced by higher levels of Wnt signaling as endochondral ossification progresses [17].

Chondrocytes derived from mesenchymal cells undergo a multistage differentiation process. Early differentiation markers of chondrocytes include sex-determining region Y (SRY)-box 9 (*Sox9*), the IIa splice form of type II collagen (*Col2a1*), aggrecan *(Agc1*), and low levels of FGF receptor 3 (*Fgfr3*), as well as specific downstream targets of the Ihh signaling pathway (Fig. 2). Flat columnar chondrocytes, which are highly proliferative, express low levels of *Runx2* and osterix (*Osx*) and high levels of *Fgfr3*, *Nkx3.2*, and protein patched homologue 1 (*Ptc1*) (Fig. 2). Next, the flat columnar chondrocytes become hypertrophic and withdraw from the cell cycle. Terminally differentiated, hypertrophic chondrocytes express type X collagen (*Col10a1*), *Runx2*, and matrix metalloproteinase 13 (*Mmp13*). MMP13 is an enzyme that degrades the cartilage matrix to support vascular invasion, which is required for bone marrow space formation (Fig. 2) [18].

Slit guidance ligands (Slits) are highly conserved in many species, and three

family members, Slit1−Slit3, have been identified [19]. The Slit proteins consist of four domains, including leucine-rich repeats (LRRs), seven to nine epidermal growth factor repeats, an amphipathic lipid-packing sensor (ALPS) domain, and a C-terminal cysteine knot. The LRR domain binds to the Ig domain of Robo isoforms and activates them. Slit-Robo signaling regulates cytoskeletal remodeling, small GTPase activity, and E-cadherin/N-cadherin/β-catenin and phosphoinositide-3-kinase (PI3K) signaling [20].

Four Robo isoforms, Robo1−Robo4, have been identified. The Slits were originally discovered as chemorepellents that controlled axon crossing in the midline of the brain [21]. However, they have been identified as key regulators of many cellular processes in multiple tissue types, including the mammary gland, heart, lung, and kidney [22][23]. A recent study showed that Slit3 also plays a role as a potent angiogenic factor and coordinates organogenesis during embryonic development [24]. Very recently, Slit3 was reported to have a novel role in bone metabolism [25], in that it synchronously stimulates bone formation and inhibits bone resorption. Slit3 was

identified as a driver of osteoclast differentiation by a secretome analysis. During osteoclast differentiation, paracrine Slit3 signaling promotes osteogenesis through the osteoblastic Robo1 and Robo2 receptors. Binding of Slit3 to the Robo1 and Robo3 receptors on osteoclasts inhibits bone resorption through inhibition of Rac GTPase. In addition, Slit3 activated β-catenin in osteoblasts to stimulate bone formation. In previous studies, global *Slit3*-defieicnt mice had congenital diaphragmatic hernia and osteopenia. In an ovariectomized osteoporosis mouse model, systemic injection of recombinant Slit3 protein restored the reduced bone mass [25].

In addition, newborn global *Slit3* knockout (KO) mice exhibited reduced skeletal growth, especially in the long bones (Fig. 3) [25]. This phenotype appeared to result from abnormal endochondral ossification. Thus, the role of Slit3 in endochondral ossification was investigated in this study.

2. Materials and Methods

2.1. Cell culture

ATDC5 cells were obtained from the Riken cell bank (Riken BioResource Research Center, Japan). ATDC5 cells were maintained in DMEM/F12 (Gibco/ThermoFisher Scientific, MA, USA) supplemented with 5% fetal bovine serum (FBS; Gibco), 100 U/ml penicillin-streptomycin (Gibco), transferrin (5 μg/ml), and selenous acid (5 ng/ml) (BD Biosciences, NJ, USA). Cells were maintained at 37°C in a humidified atmosphere of 5% CO_2. To induce chondrocyte differentiation, cells were cultured in ITS medium supplemented with insulin (5 μg/ml), transferrin (5 μg/ml), and selenous acid (5 ng/ml) (Sigma-Aldrich, MO, USA). Fixed ATDC5 cells were stained with Alcian blue (pH 1.0) overnight after differentiation in ITS medium for 14 days in 12-well plates. ATDC5 cells differentiated for 7, 12, and 14 days were harvested for western blotting and qRT-PCR.

Wnt3a-producing L929 cells [26] were cultured in DMEM (Gibco) with 10% FBS and 100 U/ml penicillin-streptomycin. To obtain Wnt3a-conditioned medium,

cells were seeded into T75 culture flasks in DMEM. After the cells were confluent, the medium was replaced with DMEM with 2% FBS, and the cells were incubated for an additional 2 days. Supernatants were filtered through a 0.45 μm filter and stored at -80°C.

2.2. Animal models

All *in vivo* experiments and protocols were approved by the Institutional Animal Care and Use Committee of the Asan Institute for Life Sciences (Seoul, South Korea). *Slit3*$^{-/-}$ [25] and *Robo2*$^{-/-}$ mice were purchased from the Mutant Mouse Regional Resource center at the University of Missouri (MMRRC; MO, USA). In each experiment, *Slit3*$^{-/-}$ and *Robo2*$^{-/-}$ mice were compared to their respective wild-type littermates. For genotyping of *Slit3*$^{-/-}$ mice, three primers were used: primer a (5′ GCG CCT CGG GCT CCT CGT GTC 3′, sense), primer b (5′ TGC GGG GGA TGC CCC GAG GAA 3′, antisense), and primer c (5′ CGG ATT CTC CGT GGG AAC AAA CGG 3′, antisense) [25]. A 250 bp genomic DNA fragment obtained using primers a and b

represented the wild-type allele, while a 410 bp genomic DNA fragment obtained using primers a and c indicated the null allele. The PCR was carried out for 35 cycles of 94°C for 30 seconds, 68.5°C for 30 seconds, and 72°C for 50 seconds.

For genotyping of *Robo2*$^{-/-}$ mice, three primers were used: primer a (5′ AAG TGC AAC GTC TCT GAA GTC CC 3′, sense), primer b (5′ GGC GGA ATT CTT AAT TAA GGC GCG 3′, antisense), and primer c (5′ TTC TTT AGA AGG CAC AAC AAT CTC AGA G 3′, antisense). A 324 bp genomic DNA fragment obtained using primers a and b represented the wild-type allele, while a 320 bp genomic DNA fragment obtained using primers a and c indicated the null allele. The PCR was carried out for 35 cycles of 94°C for 30 seconds, 63.5°C for 30 seconds, and 72°C for 1 min.

2.3. Western blot analysis

ATDC5 cells were seeded in 6-well plates. After differentiation for 7 or 12 days with ITS medium, the differentiated cells were harvested in lysis buffer [150 mM NaCl, 10 mM sodium phosphate (pH 7.2), 1 mM EDTA, 1% Na-deoxycholate, 1%

NP-40, 0.1% sodium dodecyl sulfate (SDS), 1 mM Na_3VO_4, 1 mM phenylmethylsulfonyl fluoride (PMSF), 1 mM NaF, and a protease inhibitor cocktail] for 15 min at 4°C. The concentration of protein was measured by BCA assay (Pierce Chemical Co., IL, USA). The samples (10–20 μg protein per sample) were separated by SDS-polyacrylamide gel electrophoresis (SDS-PAGE) on 12–15% gels and then transferred to nitrocellulose membranes (Amersham Biosciences, UK). The membranes were blocked with 5% skim milk in TBST [500 mM Tris-HCl (pH 7.4), 1.5 M NaCl, and 0.1% Tween-20) for 1 hour at room temperature. The membranes were incubated with primary antibodies overnight at 4°C in 5% milk, and subsequently with secondary antibodies for 1 hour at room temperature [25]. The antibodies used were: anti-collagen II (Col2a1) (NB100-91715, Novus Biologicals, CO, USA), anti-collagen X (Col10a1) (ab58632, Abcam, UK), anti-Sox9 (82630S, Cell Signaling, MA, USA), anti-vascular endothelial growth factor (VEGF) (ab46154, Abcam), anti-MMP13 (ab39012, Abcam), anti-Robo1 (ab7279, Abcam), anti-Robo2 (RP2861, ECM, KY, USA), anti-Robo3 (ab101811, Abcam), anti-Robo4 (ab10547, Abcam), and anti-

β-actin (A2228, Sigma-Aldrich). Immuno-complexes were visualized by enhanced chemiluminescence (PerkinElmer, MA, USA).

2.4. Quantitative reverse-transcription PCR (qRT-PCR)

Total RNA was isolated using TRIzol reagent (Invitrogen/ThermoFisher Scientific) according to the manufacturer's protocol. First-strand cDNA was synthesized from 5 μg of total RNA using the Superscript III First-Strand Synthesis System (Invitrogen) with oligo dT primers. The Biometra thermal cycler (Göttingen, Germany) was used for all PCR amplification reactions. Quantitative RT-PCR was performed on a Light Cycler 480 (Roche, Switzerland) with Probes Master Mix (Roche) and Light Cycler 480 SYBR Green I Master Mix (Roche). The threshold cycle (Ct) values for each gene were normalized to the Ct values of 18S RNA. The specific probes were Mm00468869_m1, Mm00448840_m1, Mm01309565_m1, Mm00487041_m1, Mm00439491_m1, and Mm01281449_m1 for *Hif1a, Sox9*,

C*ol2a1*, C*ol10a1*, *Mmp13*, and *Vegf*, respectively. The specific primers were 5′ CAT GAG AGA GGC GAA TGG AA 3′ (sense) and 5′ TGA TCT CGT AGC GAT CTT TCT TCT 3′ (antisense) for *Agc1*, 5′ AGC CCC ACA CAA ACA AGG 3′ (sense) and 5′ AAG CTG GGC TTG CTG TAG G 3′ (antisense) for *Robo2*, and 5′ CTC AAC ACG GGA AAC CTC AC 3′ (sense) and 5′ CGC TCC ACC AAC TAA GAA CG 3′ (antisense) for *18S*. The PCR conditions were 45 cycles of 95°C for 10 seconds, 55°C for 15 seconds, and 72°C for 20 seconds.

2.5. Luciferase assay

To measure Wnt/β-catenin signaling activity, pSuper 8× TOP-Flash plasmid (plasmid #12456, Addgene, MA, USA) [27] and pRL-TK plasmid were transfected into ATDC5 cells using Lipofectamine 2000 transfection reagent (Invitrogen). After 24 hours of transfection, luciferase activity was measured by Dual-Luciferase reporter assay (Promega, WI) according to the manufacturer's instructions. Relative activity

was calculated as the ratio of the firefly luciferase reporter to the Renilla luciferase control. Luciferase activity was measured using a luminometer (Centro LB 960, Berthold Technologies, Germany).

2.6. Skeletal preparation

Newborn mice and embryos were skinned, eviscerated, and fixed in 100% ethanol for 24 hours at room temperature (RT) on a rocker. In all timed pregnancies, the plug date was defined as E0.5. The embryos were transferred to 100% acetone for 24 hours at RT on a rocker and then stained with 0.1% Alizarin red and 0.3% Alcian blue stain for 3 days at 37°C on a rocker. The embryos were then incubated in 1% KOH for a minimum of 3 hours, and then placed through a graded series of glycerol/KOH washes, gradually increasing the glycerol ratio. Finally, the embryos stored in 100% glycerol [28].

2.7. Histological analysis

Freshly dissected bones were immediately fixed in ice-cold 4% paraformaldehyde solution for 4 hours. The tissues were embedded in paraffin and sectioned at a 6 μm thickness. For phenotype analysis, samples from knockouts and wild-type littermates were always sectioned, stained, imaged, and analyzed together under the same settings and conditions. After deparaffinization, Alcian blue and von Kossa staining was performed according to standard procedures. Tartrate-resistant acid phosphatase (TRAP) (Sigma-Aldrich) and hematoxylin and eosin (H&E) (Sigma-Aldrich) staining were performed according to the manufacturer's instructions. For immunohistochemical (IHC) staining of anti-collagen II, paraffin-embedded sections were subjected to antigen retrieval in citrate buffer (pH 6.0), permeabilized for 10 min in 0.3% Triton X-100, blocked in 5% bovine serum albumin (BSA) at RT for 30 min, and incubated with primary antibody (NB100-91715, Novus Biologicals) diluted in 5% BSA in PBS for 2 hours at RT or overnight at 4°C. After primary antibody incubation, colorimetric development was performed using liquid DAB substrate (Invitrogen).

2.8. Cell viability and proliferation

Cell viability was measured using the Cell Counting Kit-8 (CCK-8; Dojindo, Japan) according to the manufacturer's instructions. Briefly, 10 μl of the CCK-8 solution was added to each well of a 96-well plate for 1 hour and the absorbance at 450 nm was measured using a microplate reader (Infinite 200 Pro; Tecan Group, Switzerland). Cell proliferation was measured by 5-bromo-2′-deoxyuridine (BrdU) incorporation (BrdU Staining Kit; Invitrogen) according to the manufacturer's protocol. Histological sections of femurs (6 μm thickness) were also immunostained for BrdU.

2.9. Statistical analyses

All *in vitro* and *in vivo* data are expressed as the mean ± standard error of the mean (SEM) of triplicate measurements from at least three independent experiments, unless otherwise specified. All statistical analyses were performed by two-tailed Student's t-test and two-way ANOVA using GraphPad Prism 7 (GraphPad Software Inc., CA). A P-value < 0.05 was considered statistically significant.

3. Results

3.1. Altered endochondral ossification in long bones of *Slit3*–deficient mice

Smaller skeletal sizes in *Slit3*$^{-/-}$ mice were presented in my previous report [25]. That finding was confirmed here, as the forelimbs and hind limbs of newborn *Slit3*$^{-/-}$ mice were 10-18% shorter in *Slit3*$^{-/-}$ mice than in their WT littermates (Fig. 4A). To determine whether embryonic long bone development was altered, histological analysis for cartilage was performed at embryonic days (E) 15.5 and 17.5 (Fig. 4B). The proliferating zones of chondrocytes were not altered, but the hypertrophic zone was significantly longer in the femurs of *Slit3*$^{-/-}$ mice at both E15.5 and E17.5, compared with WT littermates. As a result, the bone area was decreased in the *Slit3*$^{-/-}$ mice. Viewing the femurs of E15.5 and E17.5 *Slit3*$^{-/-}$ mice at higher magnification only showed enlarged hypertrophic zones and did not reveal any deterioration in bone structures (Fig. 4C).

During endochondral ossification, hypertrophic chondrocyte maturation is followed by blood vessel invasion with osteoclastic bone resorption and osteoblastic

mineralization [3]. TRAP-positive osteoclast lineage cells appeared in the femurs of WT mice at E15.5, and were more prominent at E17.5 (Fig. 5A). However, the cells were not noted in the femurs of *Slit3*$^{-/-}$ mice at E15.5, and were decreased at E17.5 compared to their WT littermates, suggesting delayed recruitment of osteoclasts into the developing bone in the *Slit3*-deficient mice. Von Kossa staining showed similar results (Fig. 5B). Mineralization of terminally differentiated chondrocytes was not noted in the *Slit3*$^{-/-}$ mice at E15.5. At the chondro-osseous junctions of E17.5 *Slit3*$^{-/-}$ femurs, mineralization had begun, but the staining was less intense than in the WT embryos.

3.2. Chondrocyte differentiation induced by Slit3

ATDC5 cells were treated with recombinant Slit3 and subjected to Alcian blue staining. Slit3 increased the Alcian blue staining intensity (Fig. 6A), suggesting that it may stimulate chondrocyte differentiation. Next, qRT-PCR was performed to evaluate the expression of marker genes related to chondrocyte differentiation (Fig. 6B). The mRNA expression of early markers, such as *Col2a1* and *Sox9*, was increased by Slit3. In particular, Slit3 induced the expression of *Col2a1*, a typical prehypertrophic marker, by two-fold compared to the untreated control after 7 days of Slit3 stimulation. The expression of late hypertrophic markers such as *Vegf, Col10a1,* and *Mmp13,* was also increased at 2 weeks. Western blotting also confirmed that Slit3 induced the expression of VEGF, Col2a1, Sox9, Col10a1, and MMP13 (Fig. 6C).

As described above, it was observed that the pattern of chondrocyte differentiation varied according to the duration of treatment with Slit3. In a follow-up experiment, ATDC5 cells were treated with Slit3 during early (days 1-7) or late (days 7-13) differentiation. The expression of differentiation markers including *Hif1a,*

Col10a1, Mmp13, Vegf, and *Sox9*, but not *Agc1*, increased when Slit3 was added during early differentiation (Fig. 6D).

In addition, the expression of these differentiation markers was assessed in the mouse long bones. IHC staining for Col2a1 was performed in the femurs of *Slit3*$^{-/-}$ mice (Fig. 6E). Its expression was decreased in the KO mice compared to their WT littermates.

By contrast, Slit3 treatment did not alter the viability (Fig. 7A) or proliferation (Fig. 7B) of ATDC5 cells. In addition, IHC staining for BrdU was performed in bone sections of *Slit3*$^{-/-}$ mice (Fig. 7C). There was no significant difference in the number of BrdU-positive proliferating chondrocytes between *Slit3*$^{-/-}$ and WT mice. These data suggest that Slit3 stimulates endochondral ossification by promoting chondrocyte differentiation without affecting chondrocyte proliferation.

3.3. Slit3 stimulates chondrocyte differentiation by inhibition of β-catenin and Robo2

Slit3 can modulate β-catenin activity, but whether it regulates it positively or negatively differs according to cell type [29][30][31][25]. Thus, it was investigated whether Slit3 affected β-catenin activity in chondrocytes. Slit3 suppressed β-catenin activity in ATDC5 cells (Fig. 8A). In addition, Slit3-induced *Mmp13* expression was reversed by pre-treatment with LiCl, which activates Wnt/β-catenin signaling by inhibition of glycogen synthase kinase (GSK)3 [32] (Fig. 8B).

Robo family members (Robo1-Robo4) are receptors for Slit family ligands [33][34]. The expression of *Robo1*, *Robo3*, and *Robo4* was not detected by qRT-PCR in ATDC5 cells (data not shown). ATDC5 cells did express Robo2, although *Robo2* mRNA expression decreased during their differentiation into mature chondrocytes (Fig. 8C). Western blot analysis also showed similar results (Fig. 8C). Lastly, knockdown of *Robo2* with siRNA completely reversed the Slit3-induced *Mmp13* expression (Fig. 8D). These data suggest that Slit3 may stimulate chondrocyte differentiation by β-

catenin suppression, and that its receptor in chondrocytes may be Robo2.

3.4. Altered endochondral ossification in the long bones of *Robo2*-deficient mice

Robo2-deficient mice were analyzed to confirm the previous data from ATDC5 cells. *Robo2*$^{-/-}$ mice were slightly smaller than the WT mice, though the difference was not as great as in *Slit3*$^{-/-}$ mice (Fig. 9A). However, there was a difference in the length of the hypertrophic zone in the long bones in *Robo2*-defieicnt mice. The hypertrophic zone was significantly longer in femurs of *Robo2*$^{-/-}$ mice at E17.5, compared to their WT littermates (Fig. 9B). Alcian blue and H&E staining of the femurs of E17.5 *Robo2*$^{-/-}$ mice did not show any deterioration in bone structures, but only showed enlarged hypertrophic zones.

4. Discussion

Slit3 is a crucial factor for endochondral ossification during embryonic bone development. Slit3 induced chondrocyte differentiation via suppression of β-catenin activity without affecting chondrocyte proliferation. Thus, in embryonic *Slit3*$^{-/-}$ and *Robo2*$^{-/-}$ mice, hypertrophic chondrocyte maturation was delayed, and, consequently, recruitment of osteoclast lineages into the hypertrophic area and subsequent mineralization were impaired, resulting in short long bones in newborn *Slit3*$^{-/-}$ mice. The receptor for Slit3 in chondrocytes was Robo2. To my knowledge, the role of the Slit/Robo system in endochondral ossification and chondrocyte biology has not been reported until now.

Previously, it was reported that Slit3 suppressed osteoclastic differentiation and stimulated osteoblastic proliferation and mobilization [25]. Here, Slit3 also regulates the differentiation of chondrocytes. In my studies, the source of Slit3 during embryonic bone development is unclear. Slit3 has been shown to be expressed in various organs in mice [34] [35] and chicks [36] during embryonic development,

including the limb buds and developing areas of the limbs as well as the ventral neural tube and sensory organs [19][37]. In particular, *Slit3* expression was restricted to the future chondrogenic core of the limb bud during early development [36]. In addition, expression of the Robo receptors, which are receptors for Slit family ligands, was also observed in the developing limbs in mice and chicks [37][38]. The expression of *Robo1* was detected in the embryonal neural tube and lung; by contrast, *Robo2* was expressed in the embryonal spinal cord, including the limb buds. These data indirectly support our finding suggesting the role of Slit3/Robo2 in the endochondral ossification.

In the present study, the role of other Slit family members such as Slit1 and Slit2 in endochondral ossification was not studied. Slit1 and Slit2 show a strong degree of homology with Slit3 - 59% and 66% in humans, and 60% and 67% in mice, respectively. In addition, the pattern of *Slit2* and *Slit3* expression during limb development is distinct [36]. For example, *Slit2* is expressed in the peripheral mesenchyme and invading muscle precursors during early development. Therefore, it is not possible to exclude the possibility that other Slit family members may also be

involved in endochondral ossification.

Slit3 enhanced chondrocyte differentiation via suppression of β-catenin activity. This is the opposite of what was observed in previous experiments with osteoblasts [25], which share a common origin with chondrocytes. Several studies have shown that Slit ligands can have either positive or negative effects on β-catenin activity depending on the cell type. For example, in osteoblasts, retinal cells, and intestinal stem cells, Slit ligands induced β-catenin activity [25][29][39]. In contrast, Slit family members suppressed β-catenin activity in lung cancer cells, breast cancer cells, and mammary stem cells [30][31]. In retinal cells in which β-catenin signaling is active, Slit/Robo signaling enhances the dissociation of β-catenin from E-cadherin through phosphorylation of β-catenin by Ab1 [25]. However, in lung cancer cells, a Slit ligand suppresses β-catenin nuclear translocation by promoting the β-catenin/E-cadherin complex at the plasma membrane [31]. Thus, it is likely that Slit/Robo signaling can differentially promote or inhibit Wnt/β-catenin signaling depending on the cellular context and the different types of receptors expressed.

A low level of β-catenin signaling activity is required for chondrocyte differentiation in osteo-chondroprogenitors [16]. During chondrogenic mesenchymal condensation, the β-catenin protein level is kept low, which enhances *Sox9* expression and suppresses *Runx2* expression to promote chondrocyte differentiation [16]. In addition, Sox9 induces degradation of β-catenin through positive feedback [40]. These findings are consistent with my current results.

Chondrocytes differentiate from mesenchymal cells. As differentiation progresses, the genes that are expressed vary [18][41]. In my study, different markers of chondrocyte differentiation were induced depending on when (in early or late differentiation) the cells were treated with Slit3. This is likely due to the fact that transcription factor expression is regulated during chondrocyte differentiation [18]. Furthermore, Slit3 regulated □-catenin at the early stage of chondrocyte differentiation. For this reason, the expression of differentiation markers in response to Slit3 treatment differed depending on when the Slit3 was added.

There were many difficulties in growing ATDC5 cells. When qRT-PCR and

western blot were performed, the ATDC5 cells harvest time varied. As the differentiation progressed, the state of the cell suddenly changed. After 10 days, the cells were dropped from the culture dish. After 14 days, the Alcian blue staining was saturated. Thus, the experiment was carried out on the 14th day, and the cells were harvested just before the cells fell from the culture dish.

In *Robo2* knockout mice, endochondral ossification was also affected. The hypertrophic zone in the long bones at E17.5 was longer in *Robo2*$^{-/-}$ mice, although the size difference was not statistically significant. This phenotype was weaker in the *Robo2*$^{-/-}$ mice than in the *Slit3*$^{-/-}$ mice. It is therefore possible that another receptors may be compensating for the *Robo2* deletion [42].

These data provides a better understanding of the role of Slit3/Robo2 signaling in chondrocyte differentiation and endochondral ossification. Chondrogenesis from MSCs is important for bone repair. After injury, MSCs migrate to the wound site, differentiate into chondrocytes, and form the callus, resulting in new bone tissue formation. Thus, our results may have implications for the development of novel

therapeutic agents for fracture healing.

5. Conclusion

In conclusion, the Slit3/Robo2 system modulated endochondral ossification during bone development, and mediated hypertrophic chondrocyte maturation via suppression of β-catenin activity. In other words, at the early stage of chondrocyte differentiation, Slit3/Robo2 signaling promotes chondrocyte differentiation through β-catenin inhibition. These data provide novel insight into the role of Slit3/Robo2 in endochondral ossification.

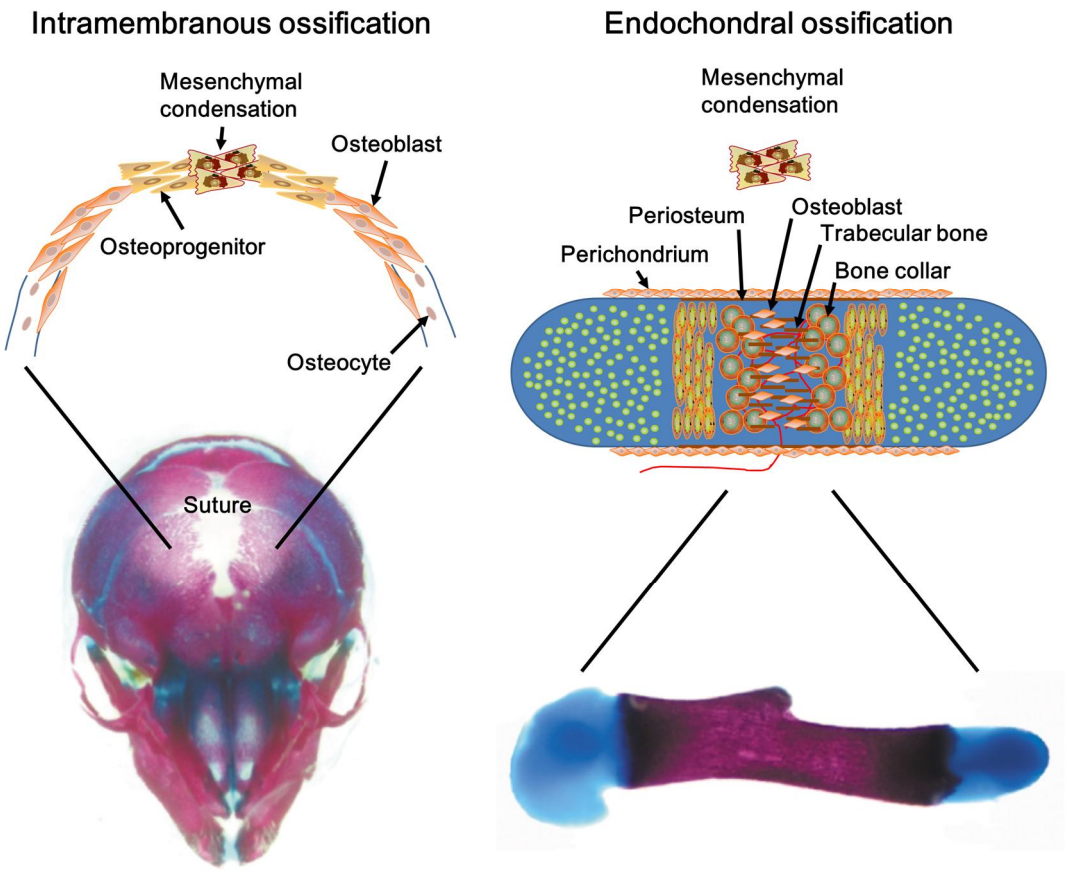

Fig. 1. Intramembranous ossification and endochondral ossification [4].

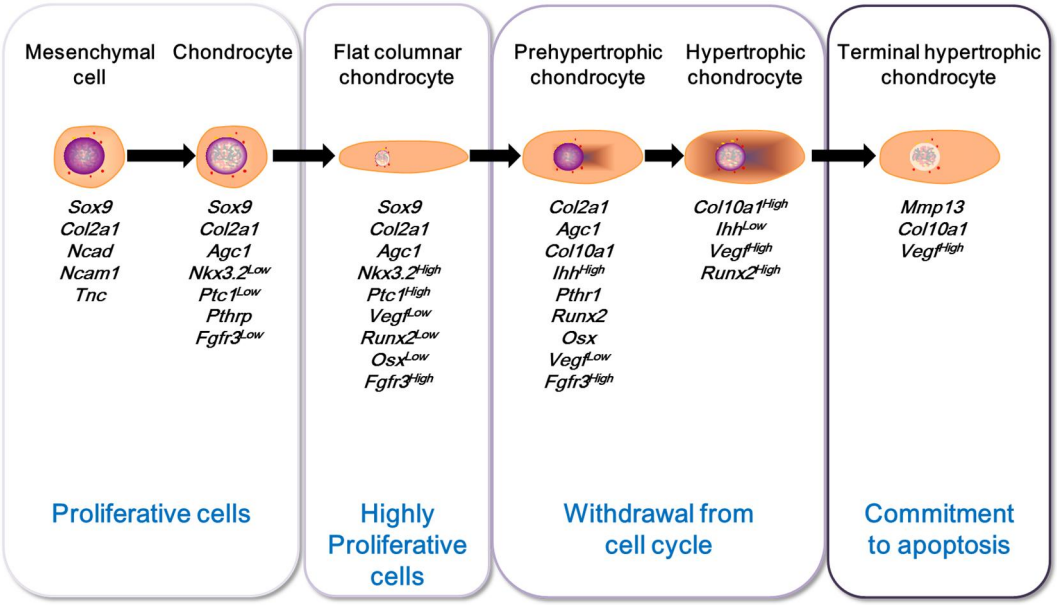

Fig. 2. Cellular events and molecular markers of chondrocyte differentiation [18].

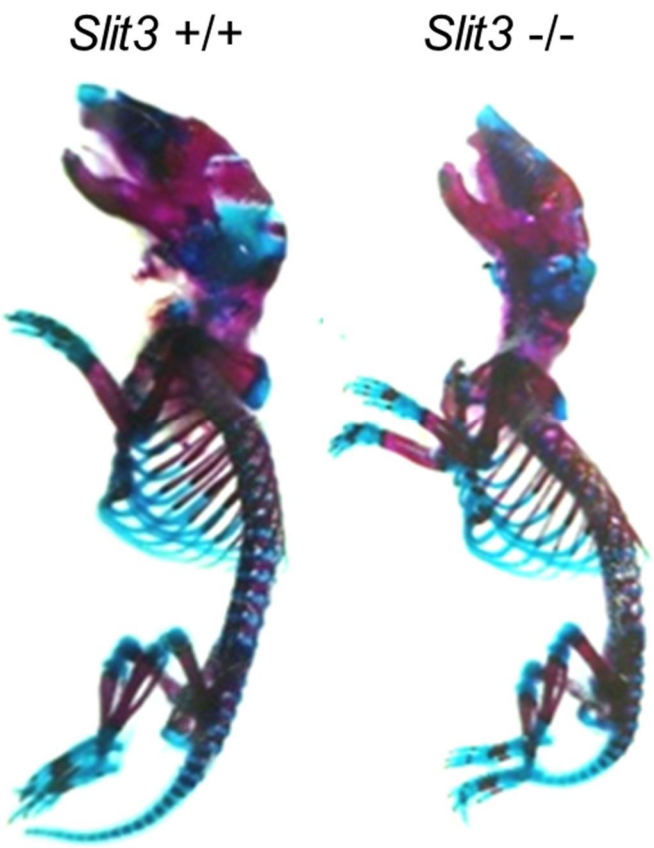

Fig. 3. Skeletal abnormalities of *Slit3*-deficient mice [25].

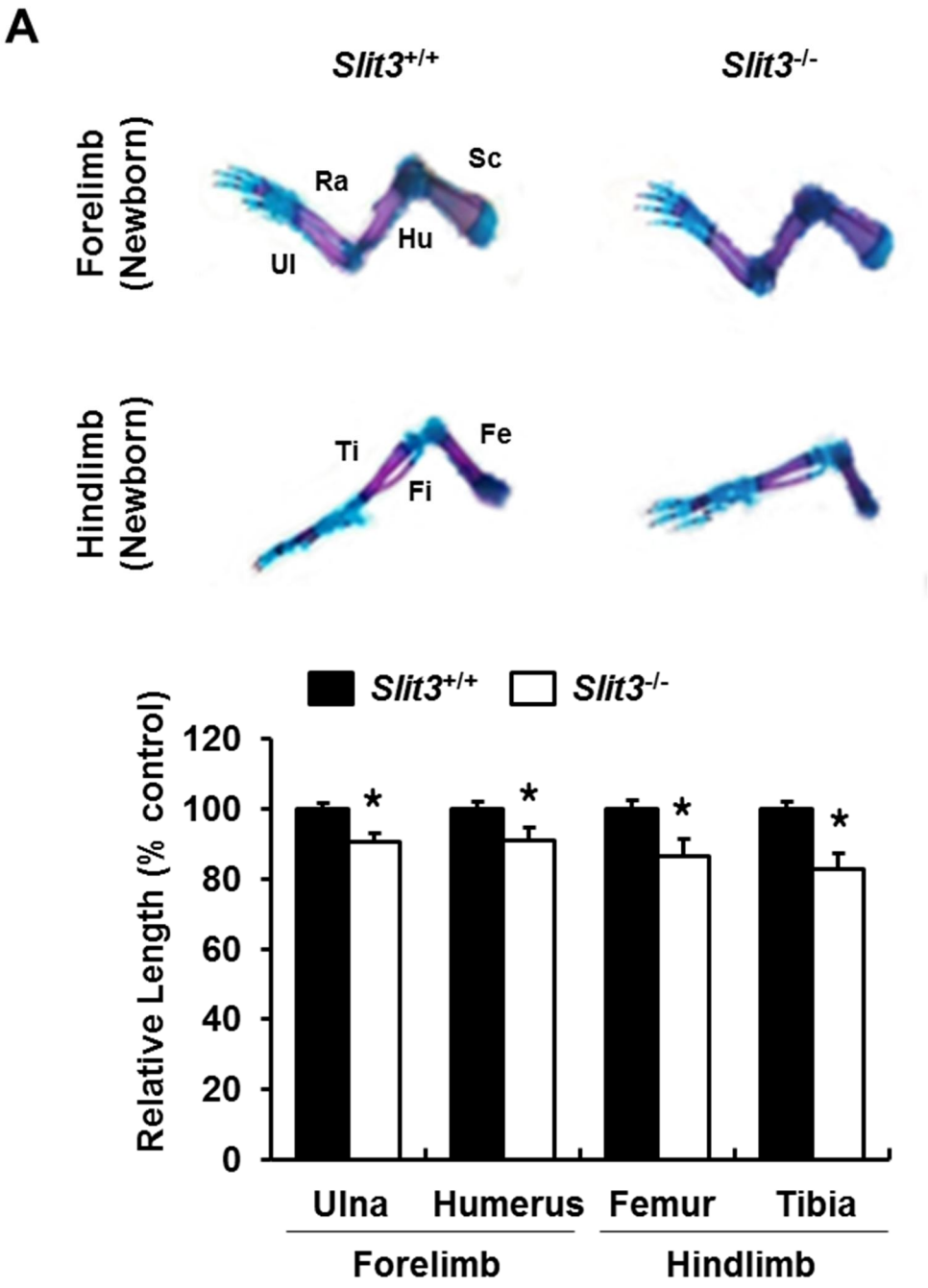
A
Slit3+/+
Slit3-/-
Forelimb (Newborn)
Ra
Sc
Hu
Ul
Hindlimb (Newborn)
Ti
Fe
Fi
Slit3+/+
Slit3-/-
Relative Length (% control)
120
100
80
60
40
20
0
*
*
*
*
Ulna
Humerus
Femur
Tibia
Forelimb
Hindlimb

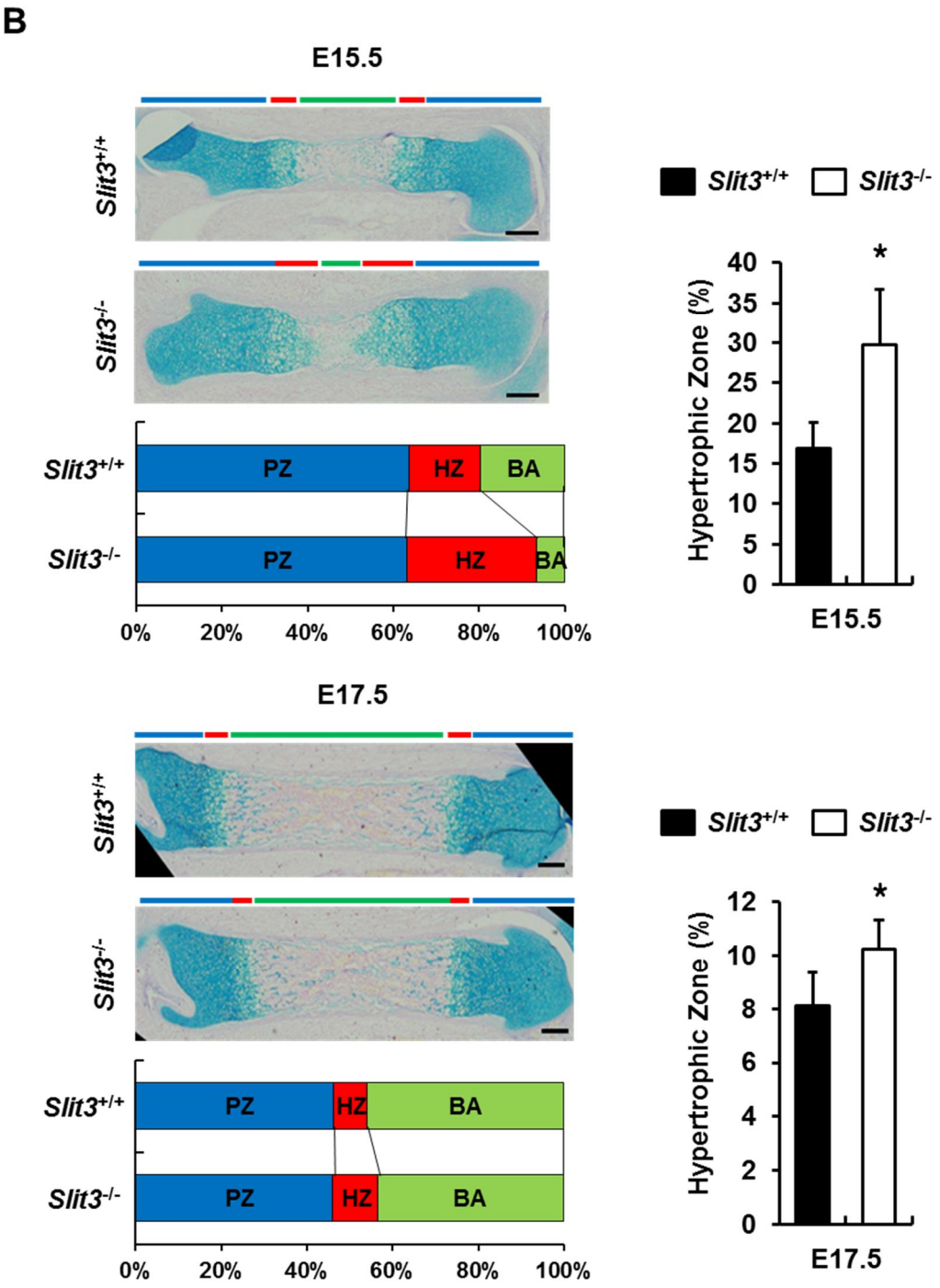
B
E15.5
Slit3+/+
Slit3-/-
PZ
HZ
BA
0%
20%
40%
60%
80%
100%
Slit3+/+
Slit3-/-
Hypertrophic Zone (%)
0
5
10
15
20
25
30
35
40
*
E15.5
E17.5
Slit3+/+
Slit3-/-
PZ
HZ
BA
0%
20%
40%
60%
80%
100%
Slit3+/+
Slit3-/-
Hypertrophic Zone (%)
0
2
4
6
8
10
12
*
E17.5

C

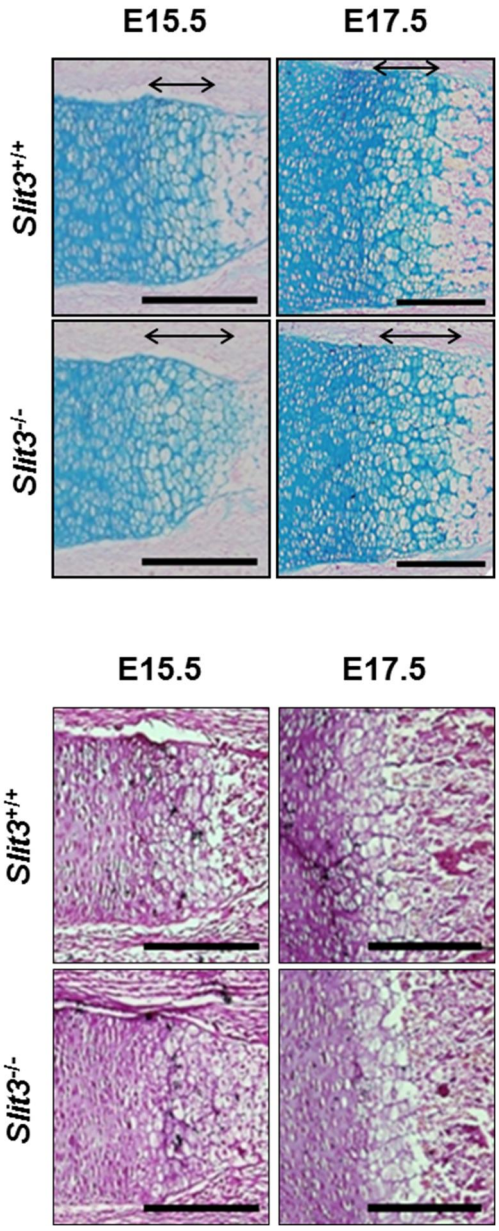

Fig. 4. Long bone phenotype in *Slit3*-deficient mice. (A) Alcian blue- and Alizarin red-stained forelimb and hind limb skeletal preparations from newborn male *Slit3*$^{+/+}$ and *Slit3*$^{-/-}$ littermates. Ra: Radius, Ul: Ulna, Hu: Humerus, Sc: Scapula, Fe: femur, Ti: Tibia, Fi: Fibula (upper panel). Quantification of the indicated bone length in newborn mice (lower panel, n = 4). (B) Alcian blue-stained femur sections at E15.5 and E17.5. Blue, red, and green bars indicate the proliferative zone (PZ), hypertrophic zone (HZ), and bone area (BA), respectively (left panel). Quantification of the hypertrophic zone length as a percentage of the total length of the femur (right panel, n = 5). (C) Analyses of the hypertrophic zone by Alcian blue staining in femur sections from *Slit3*$^{+/+}$ and *Slit3*$^{-/-}$ littermates at E15.5 and E17.5. The double-headed black arrows represent the hypertrophic zone (upper panel). Analyses of hypertrophic chondrocytes by hematoxylin and eosin (H&E) staining in femur sections from *Slit3*$^{+/+}$ and *Slit3*$^{-/-}$ littermates (lower panel). Scale bar, 200 □ m. Bars represent the mean percentages (± SEM). Statistical analyses were performed by two-tailed Student′s t-test. **P* < 0.05 vs. wild-type littermates.

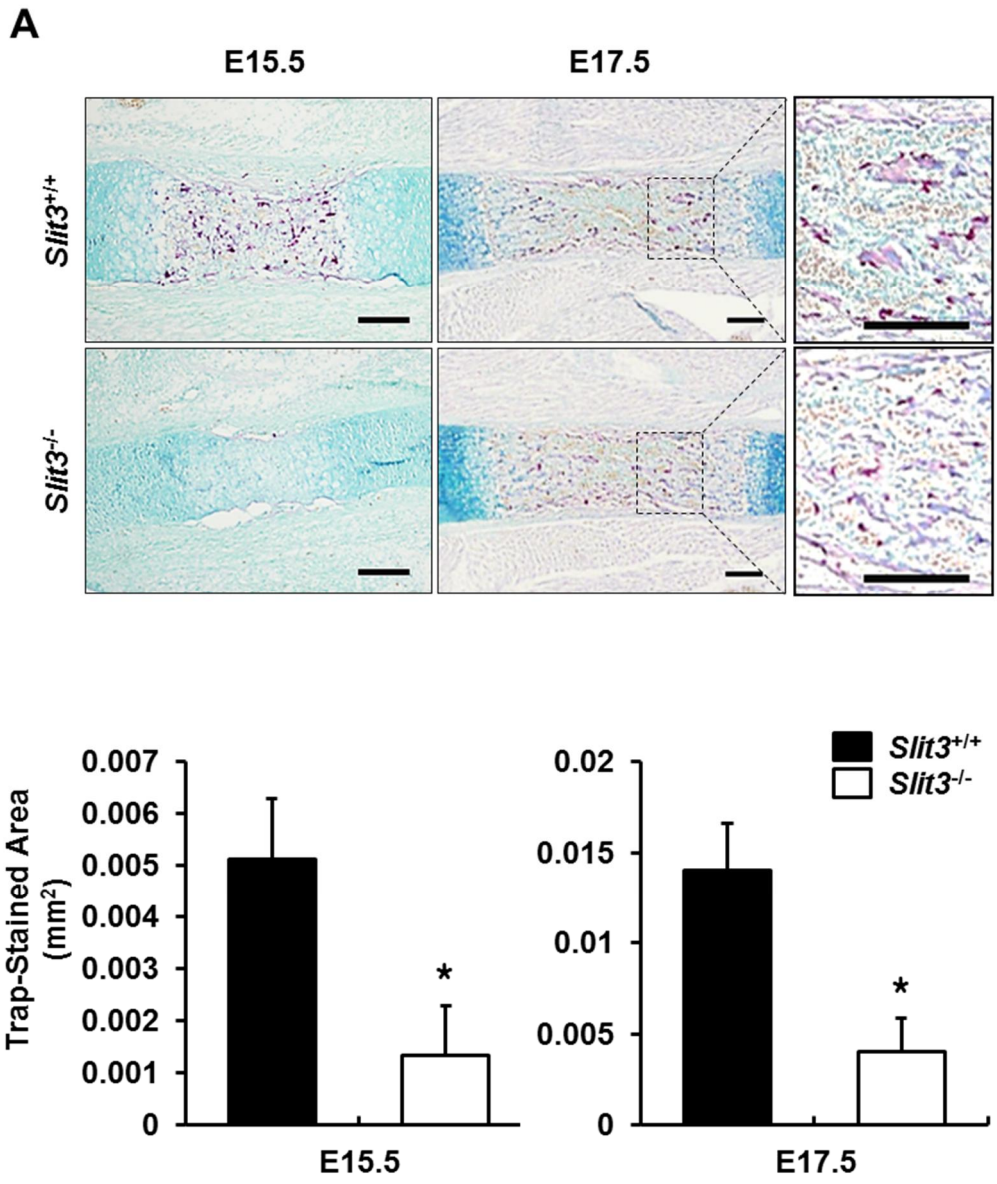
A
E15.5
E17.5
Slit3+/+
Slit3-/-
Trap-Stained Area (mm2)
0.007
0.006
0.005
0.004
0.003
0.002
0.001
0
0.02
0.015
0.01
0.005
0
*
*
E15.5
E17.5
Slit3+/+
Slit3-/-

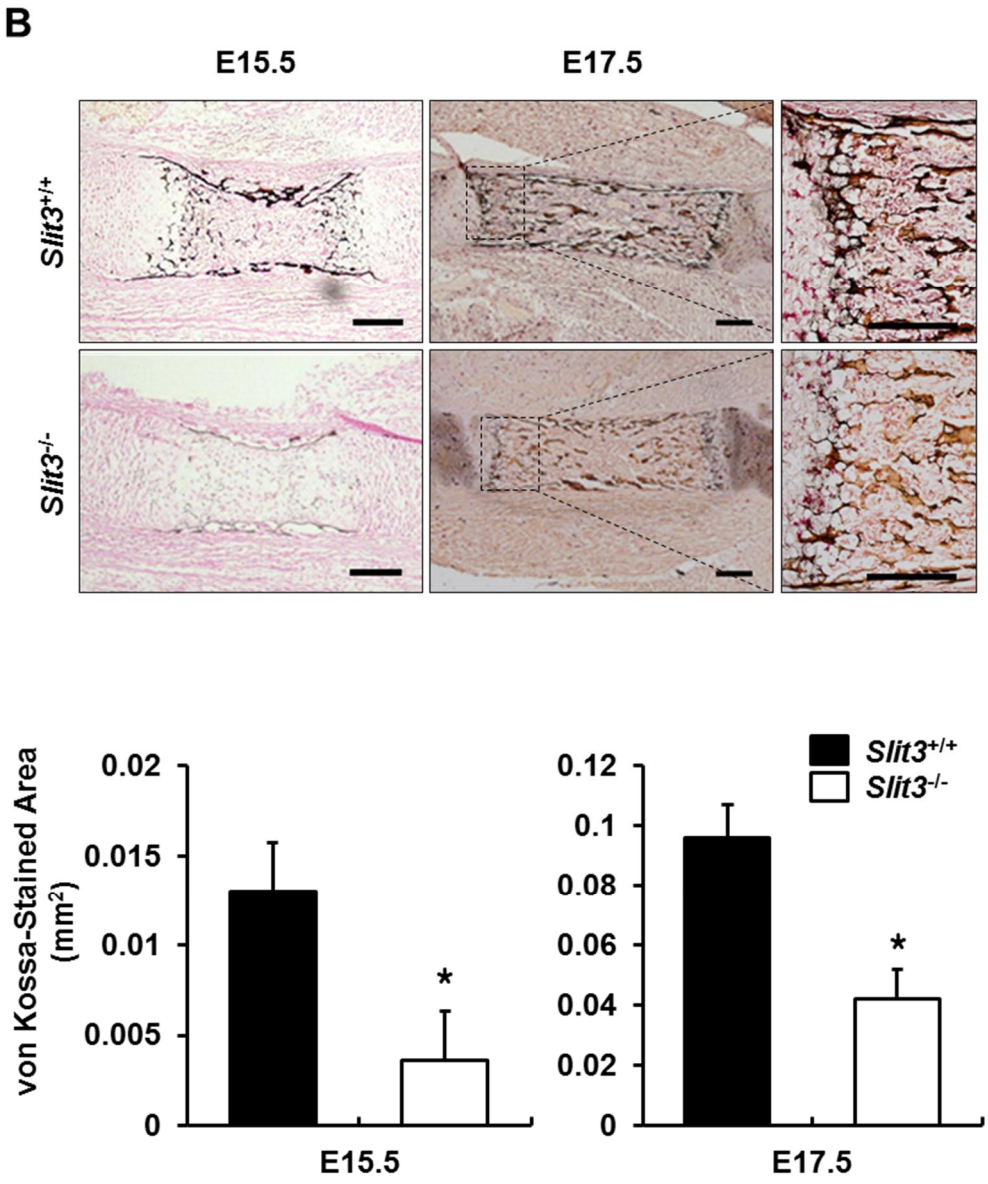
B
E15.5
E17.5
Slit3+/+
Slit3-/-
von Kossa-Stained Area (mm2)
0.02
0.015
0.01
0.005
0
*
E15.5
0.12
0.1
0.08
0.06
0.04
0.02
0
*
E17.5
Slit3+/+
Slit3-/-

Fig. 5. Delayed osteoclast recruitment and ossification in *Slit3*-deficient embryos. (A) Tartrate-resistant acid phosphatase (TRAP)-stained sections of femurs from male *Slit3*$^{+/+}$ and *Slit3*$^{-/-}$ littermates at E15.5 and E17.5 (upper panel). Quantification of the TRAP-stained area (lower panel, n = 3). (B) Von Kossa-stained sections from the same femurs (upper panel). Quantification of the von Kossa-stained area (lower panel, n = 3). Scale bar, 200 μm. Bars represent the mean percentages (± SEM). Statistical analyses were performed by two-tailed Student's t-test. **P* < 0.05 vs. wild-type littermates.

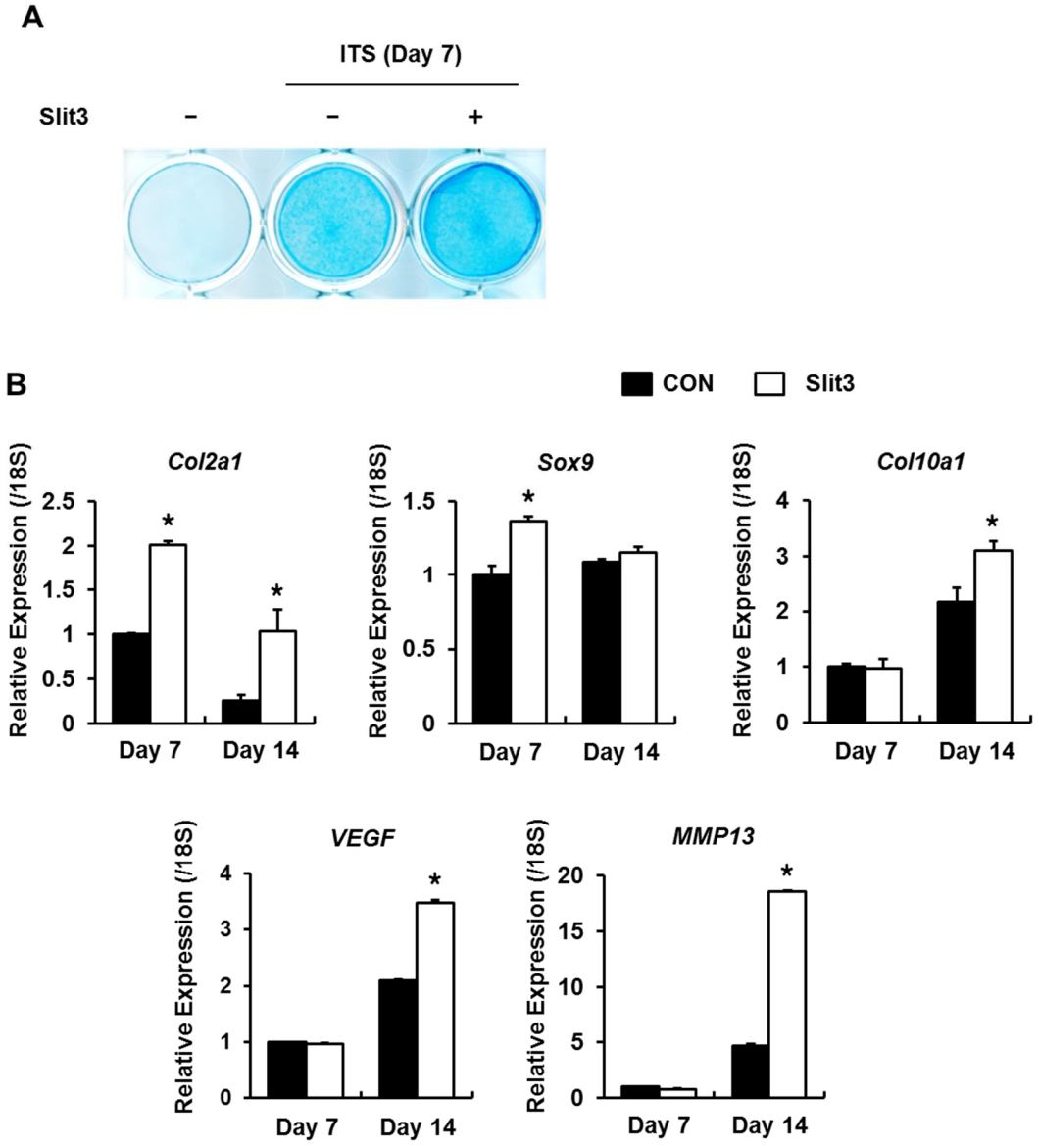
A
ITS (Day 7)
Slit3
–
–
+
B
CON
Slit3
Col2a1
Sox9
Col10a1
VEGF
MMP13
Relative Expression (/18S)
Day 7
Day 14
*

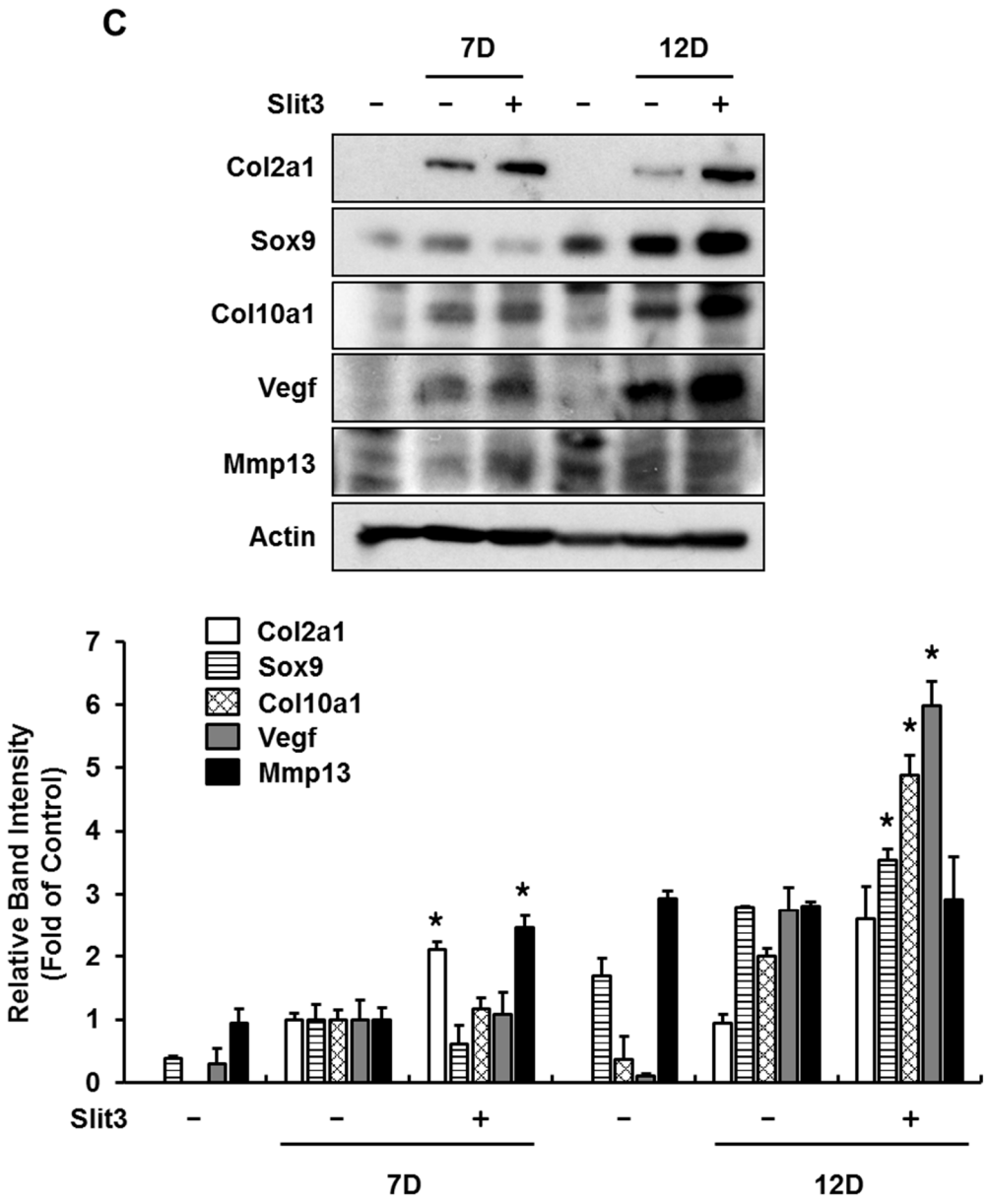
C
7D
12D
Slit3 – – + – – +
Col2a1
Sox9
Col10a1
Vegf
Mmp13
Actin
Col2a1
Sox9
Col10a1
Vegf
Mmp13
Relative Band Intensity
(Fold of Control)
0
1
2
3
4
5
6
7
*
Slit3 – – + – – +
7D
12D

D

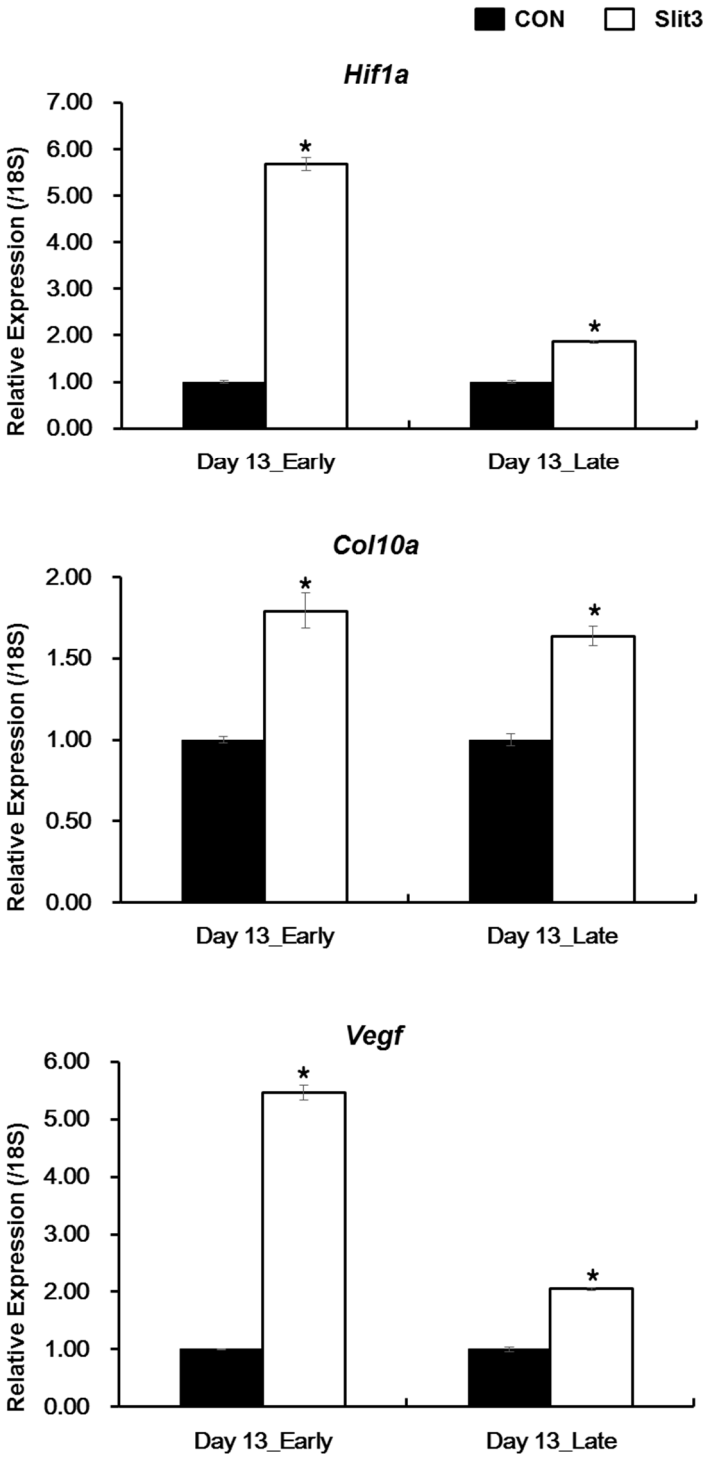
CON
Slit3
Hif1a
Relative Expression (/18S)
7.00
6.00
5.00
4.00
3.00
2.00
1.00
0.00
*
*
Day 13_Early
Day 13_Late
Col10a
Relative Expression (/18S)
2.00
1.50
1.00
0.50
0.00
*
*
Day 13_Early
Day 13_Late
Vegf
Relative Expression (/18S)
6.00
5.00
4.00
3.00
2.00
1.00
0.00
*
*
Day 13_Early
Day 13_Late

D’

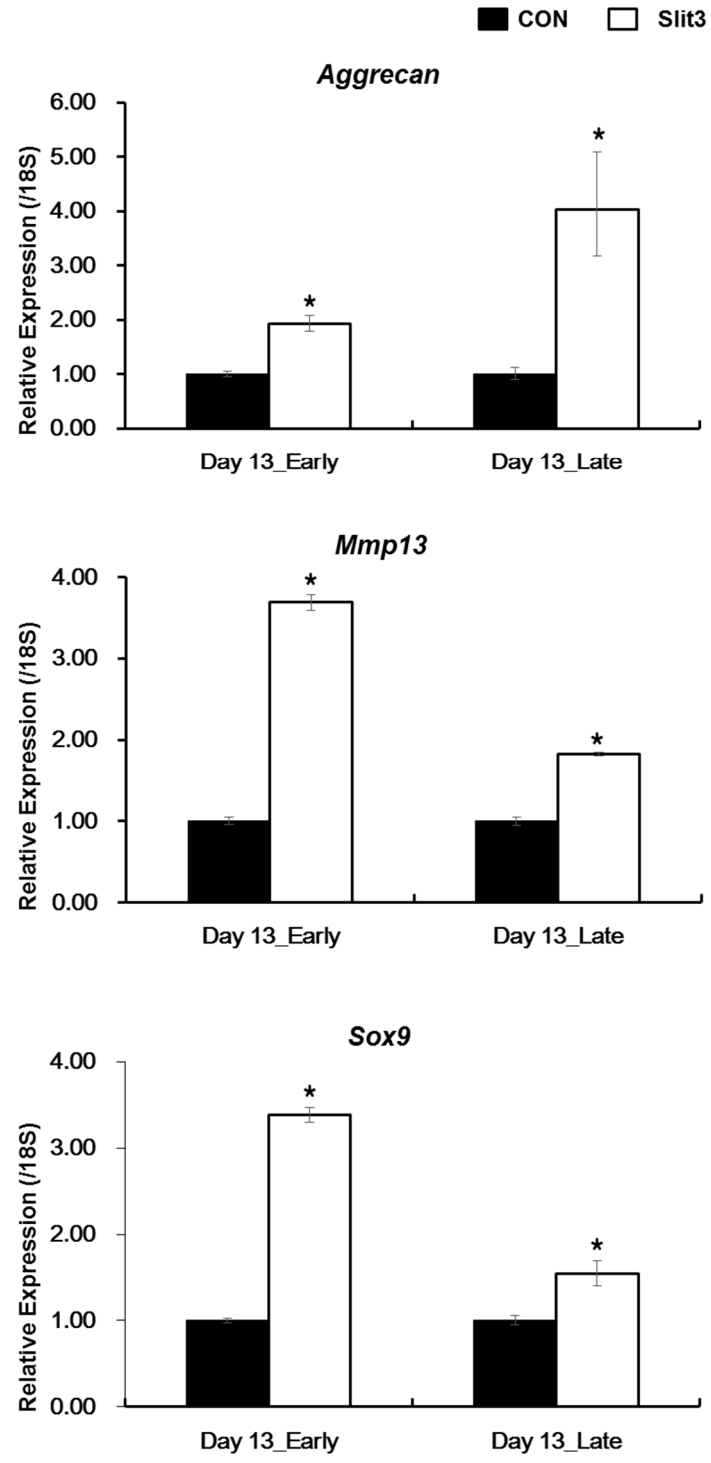
CON
Slit3
Aggrecan
Relative Expression (/18S)
6.00
5.00
4.00
3.00
2.00
1.00
0.00
*
*
Day 13_Early
Day 13_Late
Mmp13
Relative Expression (/18S)
4.00
3.00
2.00
1.00
0.00
*
*
Day 13_Early
Day 13_Late
Sox9
Relative Expression (/18S)
4.00
3.00
2.00
1.00
0.00
*
*
Day 13_Early
Day 13_Late

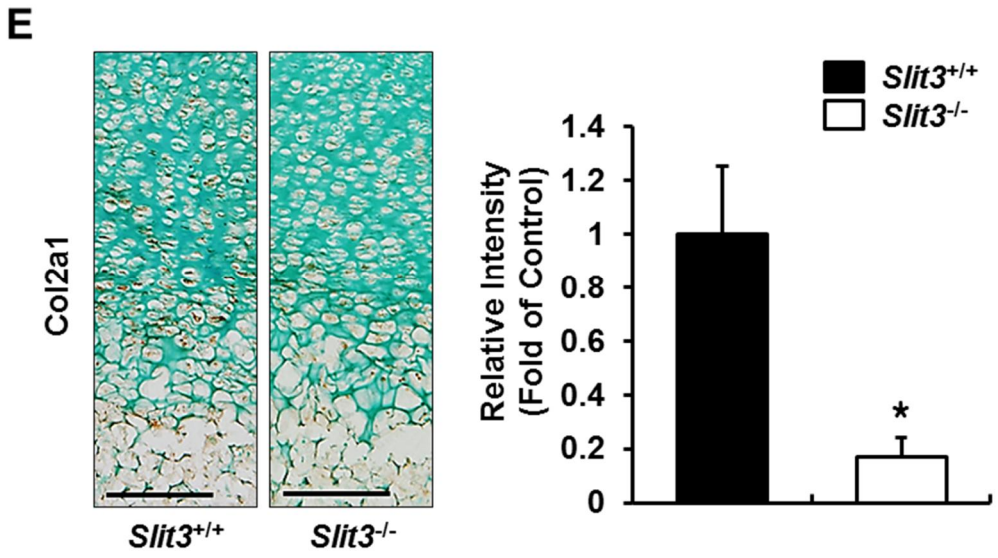
E
Col2a1
Slit3+/+
Slit3-/-
Slit3+/+
Slit3-/-
Relative Intensity
(Fold of Control)
1.4
1.2
1
0.8
0.6
0.4
0.2
0
*

Fig. 6. Enhanced chondrocyte differentiation by recombinant Slit3. (A) Alcian blue staining of ATDC5 cells with or without treatment with recombinant Slit3 (1 μg/ml). Cultured cells in 12-well plates were photographed at day 7. (B) Quantitative RT-PCR analysis for *Col2a1, Sox9*, *Col10a1, Vegf,* and *Mmp13* in chondrogenic ATDC5 cells differentiated for 7 or 14 days in the absence or presence of recombinant Slit3 (1 μg/ml). (C) Western blot analysis of Col2a1, Sox9, Col10a1, VEGF, and MMP13 in differentiated chondrogenic ATDC5 cells after 7 or 12 days of incubation in the absence or presence of recombinant Slit3 (1 μg/ml) (upper panel). Quantification of the band intensities (lower panel). (D) Quantitative RT-PCR analysis for *Hif1a, Agc1, Col10a1, Mmp13, Vegf,* and *Sox9* in chondrogenic ATDC5 cells differentiated for 13 days in the absence or presence of recombinant Slit3 (1 μg/ml). In the conditions labeled ″Early,″ Slit3 was added during early differentiation (from day 1 to day 7) and in the conditions labeled ″Late,″ Slit3 was added during late differentiation (from day 7 to day 13). (E) Col2a1 immunohistochemical staining in hypertrophic chondrocytes of femurs from male *Slit3*$^{+/+}$ and *Slit3*$^{-/-}$ mice at E17.5. Scale bar, 100 μm. Bars

represent the mean (± SEM). Statistical analyses were performed by two-tailed Student's t-test or two-way ANOVA. *$P < 0.05$ vs. untreated control or wild-type littermates.

A

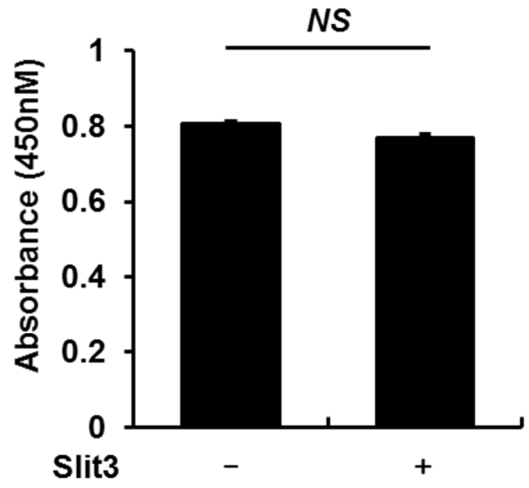
NS
Absorbance (450nM)
1
0.8
0.6
0.4
0.2
0
Slit3
–
+

B

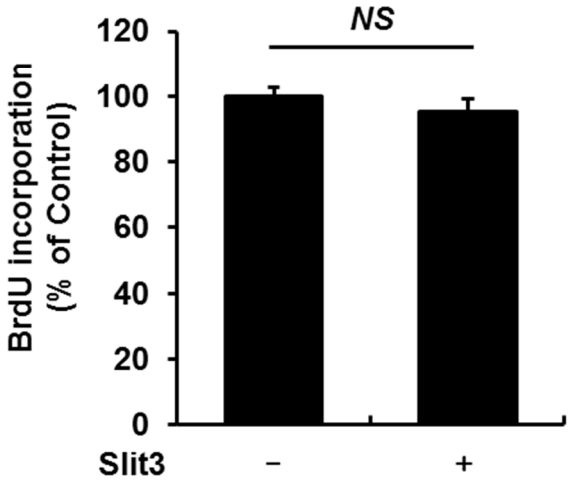
NS
BrdU incorporation
(% of Control)
120
100
80
60
40
20
0
Slit3
–
+

C

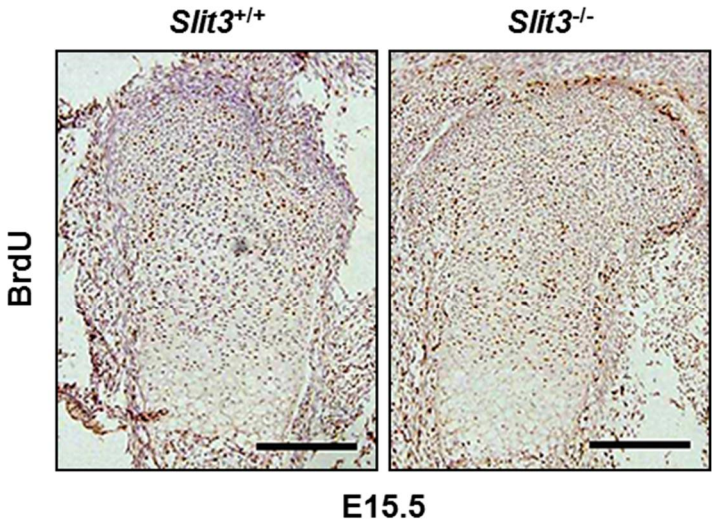
Slit3+/+
Slit3-/-
BrdU
E15.5

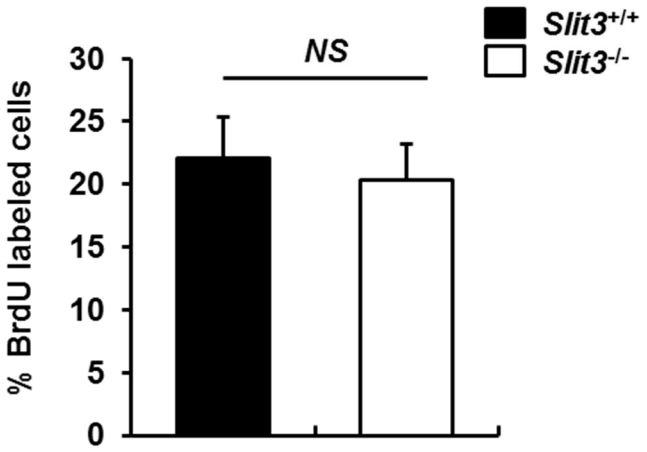
Slit3+/+
Slit3-/-
NS
% BrdU labeled cells
30
25
20
15
10
5
0

Fig. 7. Slit3 does not affect chondrocyte proliferation. (A) CCK-8 assay of chondrogenic ATDC5 cells cultured with or without Slit3 (1 μg/ml) for 48 hours. (B) BrdU incorporation assay of chondrogenic ATDC5 cells cultured with or without Slit3 (1 ug/ml) for 24 hours. (C) *In vivo* BrdU labeling in femur sections of male *Slit3*$^{+/+}$ and *Slit3*$^{-/-}$ mice at E15.5 (upper panel). Scale bar, 200 μm. Quantification of the BrdU-labeled cells in the proliferating zone of mouse femur sections (lower panel). Bars represent the mean percentages (± SEM; n = 6). Statistical analyses were performed by two-tailed Student's t-test. *NS,* not significant.

A

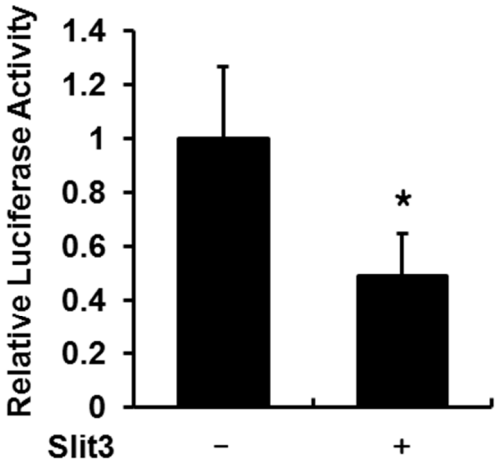
Relative Luciferase Activity
1.4
1.2
1
0.8
0.6
0.4
0.2
0
*
Slit3
–
+

B

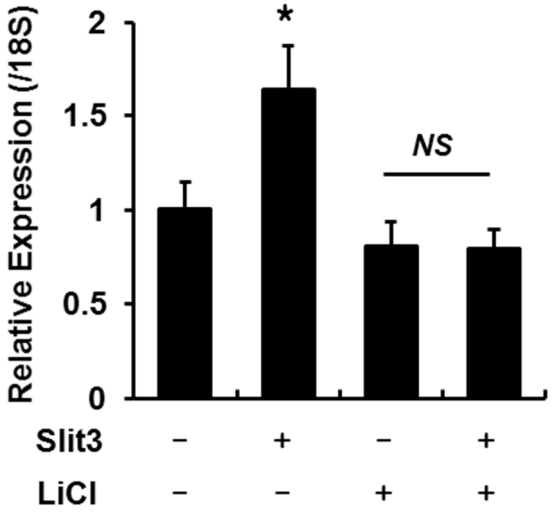
Relative Expression (/18S)
2
1.5
1
0.5
0
*
NS
Slit3
–
+
–
+
LiCl
–
–
+
+

C

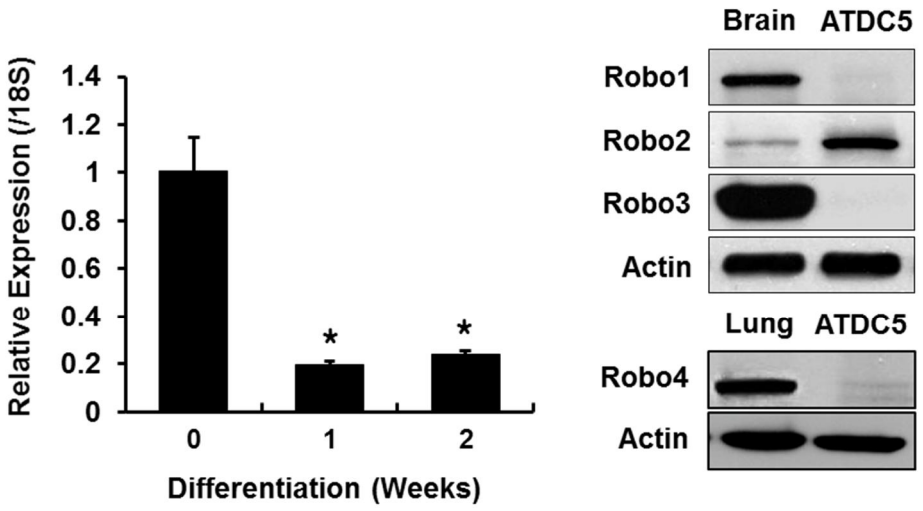
Relative Expression (/18S)
1.4
1.2
1
0.8
0.6
0.4
0.2
0
*
*
0
1
2
Differentiation (Weeks)
Brain
ATDC5
Robo1
Robo2
Robo3
Actin
Lung
ATDC5
Robo4
Actin

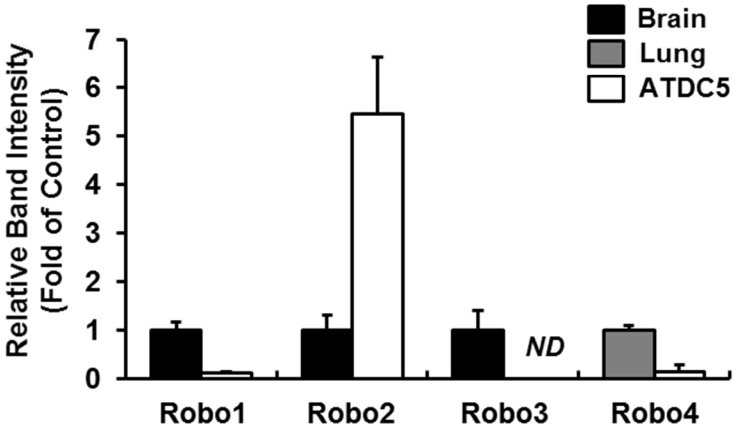
Relative Band Intensity
(Fold of Control)
7
6
5
4
3
2
1
0
Brain
Lung
ATDC5
ND
Robo1
Robo2
Robo3
Robo4

D

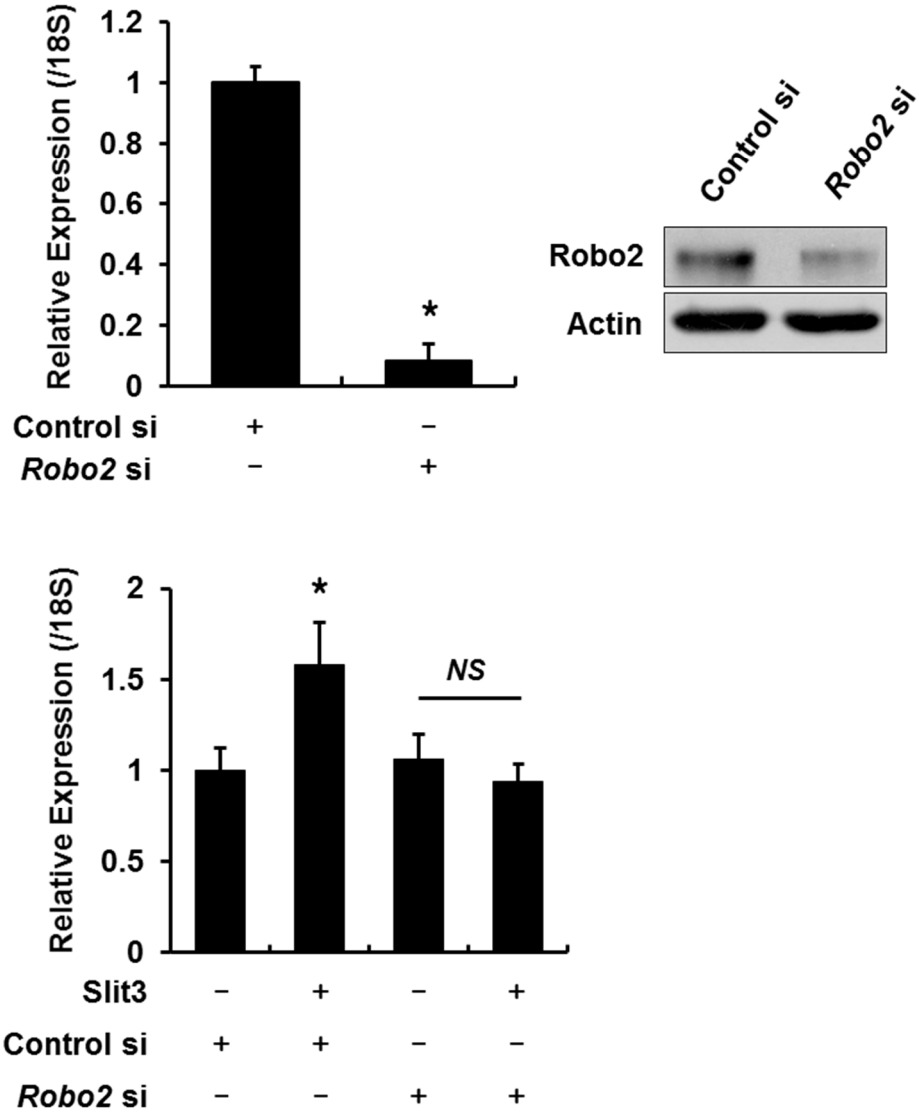
Relative Expression (/18S)
1.2
1
0.8
0.6
0.4
0.2
0
*
Control si
Robo2 si
Robo2
Actin
Control si + −
Robo2 si − +
Relative Expression (/18S)
2
1.5
1
0.5
0
*
NS
Slit3 − + − +
Control si + + − −
Robo2 si − − + +

Fig. 8. Wnt/β-catenin signaling and the Robo2 receptor are involved in accelerated chondrogenesis by Slit3. (A) Super TOP-Flash luciferase reporter assay of ATDC5 cells cultured in the absence or presence of recombinant Slit3 (1 μg/ml) for 24 hours. (B) Quantitative RT-PCR analysis of *Mmp13* mRNA in ATDC5 cells differentiated for 10 days with or without recombinant Slit3 (1 μg/ml) in the presence of LiCl (10 mM). (C) Quantitative RT-PCR analysis of *Robo2* mRNA from ATDC5 cells after 7 or 14 days of differentiation (left panel). Western blot analysis for Robo1-4 in ATDC5 cells. Mouse brain and lung tissues were used as positive controls. Quantification of the band intensities of the expressed proteins (lower panel). (D) Quantitative RT-PCR and Western blot analyses to determine the efficiency of *Robo2* knockdown in ATDC5 cells (upper panel). Quantitative RT-PCR analysis of *Mmp13* expression in chondrogenic ATDC5 cells differentiated for 10 days with or without recombinant Slit3 (1 μg/ml) (lower panel). Bars represent the mean value (± SEM). Statistical analyses were performed by two-tailed Student's t-test or two-way ANOVA. **P* < 0.05 vs. untreated control. *NS*, not significant. *ND*, not detected.

A

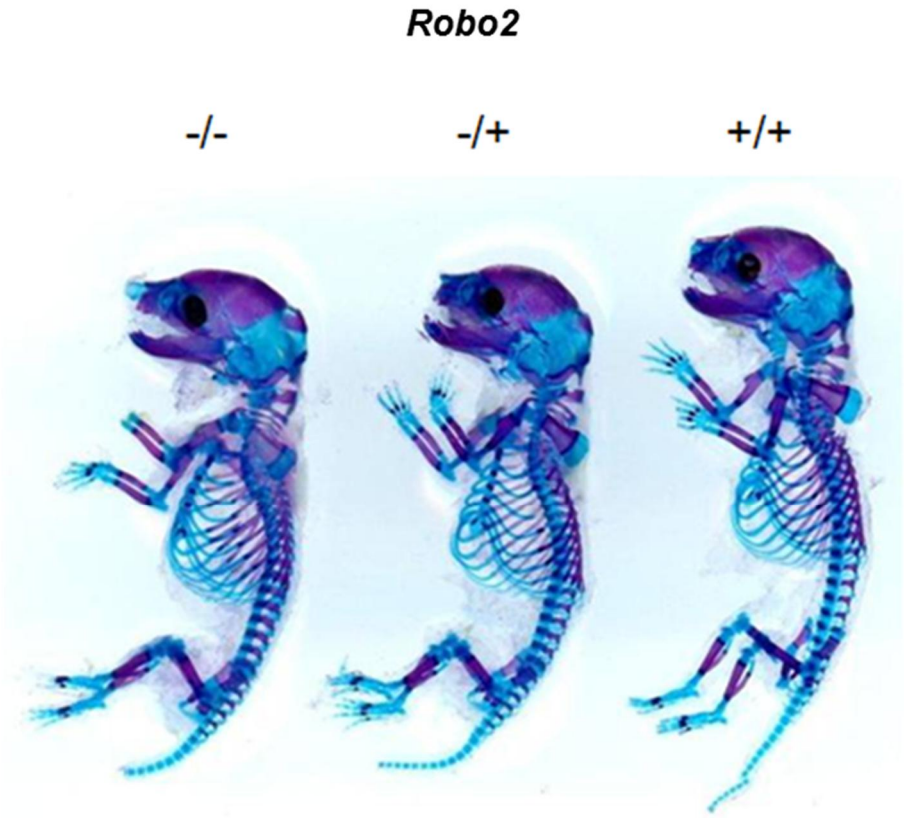

B

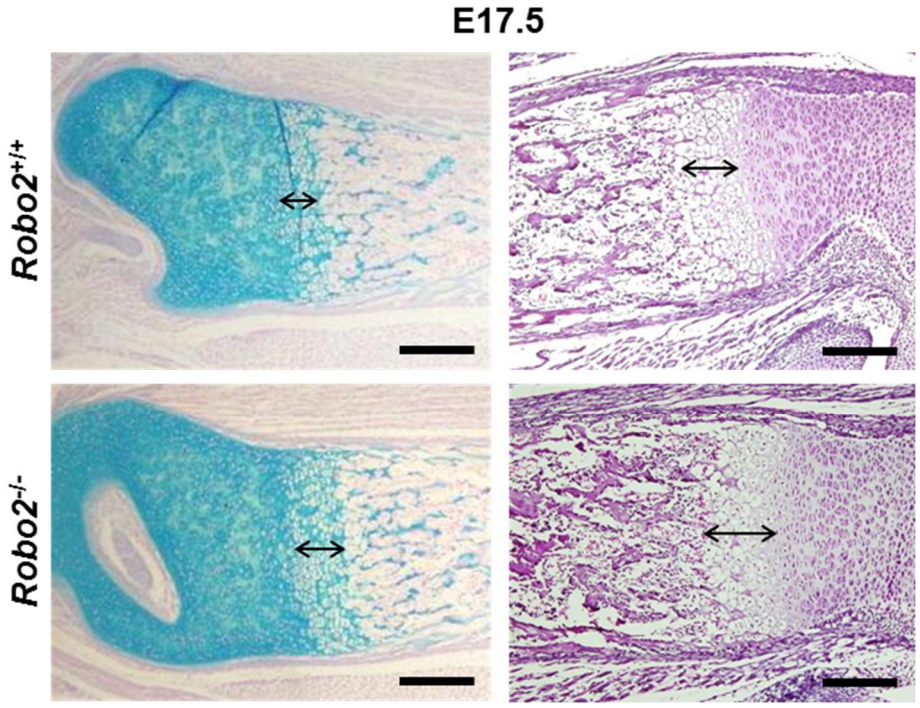

Fig. 9. Skeletal abnormalities of *Robo2*-deificient mice. (A) Alcian blue and Alizarin red staining of newborn *Robo2*$^{+/+}$, *Robo2*$^{+/-}$, and *Robo2*$^{-/-}$ littermates. (B) Analyses of the hypertrophic zones by Alcian blue staining in femur sections from *Robo2*$^{+/+}$ and *Robo2*$^{-/-}$ littermates at E17.5. The black double-headed arrows represent the hypertrophic zone (left panel). Analyses of hypertrophic chondrocytes by hematoxylin and eosin (H&E) staining in femur sections from *Robo2*$^{+/+}$ and *Robo2*$^{-/-}$ littermates (right panel). Scale bar, 200 μm.

References

[1] B.R. Olsen, A.M. Reginato, W. Wang, BONE DEVELOPMENT, 2000. www.annualreviews.org (accessed October 31, 2018).

[2] E. Kozhemyakina, A.B. Lassar, E. Zelzer, A pathway to bone: signaling molecules and transcription factors involved in chondrocyte development and maturation., Development. 142 (2015) 817–31. doi:10.1242/dev.105536.

[3] N. Ortega, D.J. Behonick, Z. Werb, Matrix remodeling during endochondral ossification, Trends Cell Biol. 14 (2004) 86–93. doi:10.1016/J.TCB.2003.12.003.

[4] K. Nakashima, B. de Crombrugghe, Transcriptional mechanisms in osteoblast differentiation and bone formation, Trends Genet. 19 (2003) 458–466. doi:10.1016/S0168-9525(03)00176-8.

[5] J.L. Ford, D.E. Robinson, B.E. Scammell, Endochondral ossification in fracture callus during long bone repair: The localisation of "cavity-lining cells" within the cartilage, J. Orthop. Res. 22 (2004) 368–375.

doi:10.1016/j.orthres.2003.08.010.

[6] J. Yang, P. Andre, L. Ye, Y.Z. Yang, The Hedgehog signalling pathway in bone formation, Int. J. Oral Sci. 7 (2015) 73–79. doi:10.1038/ijos.2015.14.

[7] C.M. Leonard, H.M. Fuld, D.A. Frenz, S.A. Downie, J. Massague, S.A. Newman, Role of transforming growth factor-β in chondrogenic pattern formation in the embryonic limb: Stimulation of mesenchymal condensation and fibronectin gene expression by exogenenous TGF-β and evidence for endogenous TGF-β-like activity, Dev. Biol. 145 (1991) 99–109. doi:10.1016/0012-1606(91)90216-P.

[8] U.I. Chung, B. Lanske, K. Lee, E. Li, H. Kronenberg, The parathyroid hormone/parathyroid hormone-related peptide receptor coordinates endochondral bone development by directly controlling chondrocyte differentiation., Proc. Natl. Acad. Sci. U. S. A. 95 (1998) 13030–5. http://www.ncbi.nlm.nih.gov/pubmed/9789035 (accessed October 10, 2018).

[9] D. Duprez, E.J. Esther, M.K. Richardson, C.W. Archer, L. Wolpert, P.M.

Brickell, P.H. Francis-West, Overexpression of BMP-2 and BMP-4 alters the size and shape of developing skeletal elements in the chick limb, Mech. Dev. 57 (1996) 145–157. doi:10.1016/0925-4773(96)00540-0.

[10] J.A. Rudnicki, A.M.C. Brown, Inhibition of chondrogenesis by Wnt gene expression in vivo and in vitro, Dev. Biol. 185 (1997) 104–118. doi:10.1006/dbio.1997.8536.

[11] S. Ohba, Hedgehog Signaling in Endochondral Ossification, J. Dev. Biol. 4 (2016) 20. doi:10.3390/jdb4020020.

[12] M. D'Angelo, D.P. Sarment, P.C. Billings, M. Pacifici, Activation of Transforming Growth Factor β in Chondrocytes Undergoing Endochondral Ossification, J. Bone Miner. Res. 16 (2001) 2339–2347. doi:10.1359/jbmr.2001.16.12.2339.

[13] U.I. Chung, B. Lanske, K. Lee, E. Li, H. Kronenberg, The parathyroid hormone/parathyroid hormone-related peptide receptor coordinates endochondral bone development by directly controlling chondrocyte

differentiation., Proc. Natl. Acad. Sci. U. S. A. 95 (1998) 13030–5. http://www.ncbi.nlm.nih.gov/pubmed/9789035 (accessed October 31, 2018).

[14] E. Minina, H.M. Wenzel, C. Kreschel, S. Karp, W. Gaffield, A.P. McMahon, A. Vortkamp, BMP and Ihh/PTHrP signaling interact to coordinate chondrocyte proliferation and differentiation., Development. 128 (2001) 4523–34. http://www.ncbi.nlm.nih.gov/pubmed/11714677 (accessed October 10, 2018).

[15] Y. Yang, Wnt signaling in development and disease., Cell Biosci. 2 (2012) 14. doi:10.1186/2045-3701-2-14.

[16] T.F. Day, X. Guo, L. Garrett-Beal, Y. Yang, Wnt/beta-catenin signaling in mesenchymal progenitors controls osteoblast and chondrocyte differentiation during vertebrate skeletogenesis., Dev. Cell. 8 (2005) 739–50. doi:10.1016/j.devcel.2005.03.016.

[17] T.P. Hill, D. Später, M.M. Taketo, W. Birchmeier, C. Hartmann, Canonical Wnt/$β$-Catenin Signaling Prevents Osteoblasts from Differentiating into

Chondrocytes, Dev. Cell. 8 (2005) 727–738.

doi:10.1016/J.DEVCEL.2005.02.013.

[18] M.J. Zuscik, M.J. Hilton, X. Zhang, D. Chen, R.J. O'Keefe, Regulation of chondrogenesis and chondrocyte differentiation by stress, J. Clin. Invest. 118 (2008) 429–438. doi:10.1172/JCI34174.

[19] W. Yuan, L. Zhou, J. hui Chen, J.Y. Wu, Y. Rao, D.M. Ornitz, The mouse SLIT family: Secreted ligands for ROBO expressed in patterns that suggest a role in morphogenesis and axon guidance, Dev. Biol. 212 (1999) 290–306. doi:10.1006/dbio.1999.9371.

[20] R.E. Dickinson, W.C. Duncan, The SLIT–ROBO pathway: a regulator of cell function with implications for the reproductive system, REPRODUCTION. 139 (2010) 697–704. doi:10.1530/REP-10-0017.

[21] T. Kidd, K.S. Bland, C.S. Goodman, Slit is the midline repellent for the Robo receptor in Drosophila, Cell. 96 (1999) 785–794. doi:10.1016/S0092-8674(00)80589-9.

[22] H. Macias, A. Moran, Y. Samara, M. Moreno, J.E. Compton, G. Harburg, P. Strickland, L. Hinck, SLIT/ROBO1 Signaling Suppresses Mammary Branching Morphogenesis by Limiting Basal Cell Number, Dev. Cell. 20 (2011) 827–840. doi:10.1016/J.DEVCEL.2011.05.012.

[23] U. Grieshammer, L. Ma, A.S. Plump, F. Wang, M. Tessier-Lavigne, G.R. Martin, SLIT2-Mediated ROBO2 signaling restricts kidney induction to a single site, Dev. Cell. 6 (2004) 709–717. doi:10.1016/S1534-5807(04)00108-X.

[24] B. Zhang, U.M. Dietrich, J.G. Geng, R. Bicknell, J.D. Esko, L. Wang, Repulsive axon guidance molecule Slit3 is a novel angiogenic factor, Blood. 114 (2009) 4300–4309. doi:10.1182/blood-2008-12-193326.

[25] B.J. Kim, Y.S. Lee, S.Y. Lee, W.Y. Baek, Y.J. Choi, S.A. Moon, S.H. Lee, J.E. Kim, E.J. Chang, E.Y. Kim, J. Yoon, S.W. Kim, S.H. Ryu, S.K. Lee, J.A. Lorenzo, S.H. Ahn, H. Kim, K.U. Lee, G.S. Kim, J.M. Koh, Osteoclast-secreted SLIT3 coordinates bone resorption and formation, J. Clin. Invest. 128

(2018) 1429–1441. doi:10.1172/JCI91086.

[26] K. Willert, J.D. Brown, E. Danenberg, A.W. Duncan, I.L. Weissman, T. Reya, J.R. Yates, R. Nusse, Wnt proteins are lipid-modified and can act as stem cell growth factors, Nature. 423 (2003) 448–452. doi:10.1038/nature01611.

[27] M.T. Veeman, D.C. Slusarski, A. Kaykas, S.H. Louie, R.T. Moon, Zebrafish prickle, a modulator of noncanonical Wnt/Fz signaling, regulates gastrulation movements., Curr. Biol. 13 (2003) 680–5.

[28] M.J. McLeod, Differential staining of cartilage and bone in whole mouse fetuses by alcian blue and alizarin red S, Teratology. 22 (1980) 299–301. doi:10.1002/tera.1420220306.

[29] J. Rhee, T. Buchan, L. Zukerberg, J. Lilien, J. Balsamo, Cables links Robo-bound Abl kinase to N-cadherin-bound beta-catenin to mediate Slit-induced modulation of adhesion and transcription., Nat. Cell Biol. 9 (2007) 883–92. doi:10.1038/ncb1614.

[30] R.C. Tseng, S.H. Lee, H.S. Hsu, B.H. Chen, W.C. Tsai, C. Tzao, Y.C. Wang,

SLIT2 attenuation during lung cancer progression deregulates β-catenin and E-cadherin and associates with poor prognosis, Cancer Res. 70 (2010) 543–551. doi:10.1158/0008-5472.CAN-09-2084.

[31] A. Prasad, V. Paruchuri, A. Preet, F. Latif, R.K. Ganju, Slit-2 induces a tumor-suppressive effect by regulating β-catenin in breast cancer cells, J. Biol. Chem. 283 (2008) 26624–26633. doi:10.1074/jbc.M800679200.

[32] V. Stambolic, L. Ruel, J.R. Woodgett, Lithium inhibits glycogen synthase kinase-3 activity and mimics Wingless signalling in intact cells, Curr. Biol. 6 (1996) 1664–1669. doi:10.1016/S0960-9822(02)70790-2.

[33] L. Huminiecki, M. Gorn, S. Suchting, R. Poulsom, R. Bicknell, Magic roundabout is a new member of the roundabout receptor family that is endothelial specific and expressed at sites of active angiogenesis, Genomics. 79 (2002) 547–552. doi:10.1006/geno.2002.6745.

[34] K. Brose, K.S. Bland, H.W. Kuan, D. Arnott, W. Henzel, C.S. Goodman, M. Tessier-Lavigne, T. Kidd, Slit proteins bind robo receptors and have an

evolutionarily conserved role in repulsive axon guidance, Cell. 96 (1999) 795–806. doi:10.1016/S0092-8674(00)80590-5.

[35] K.H. Wang, K. Brose, D. Arnott, T. Kidd, C.S. Goodman, W. Henzel, M. Tessier-Lavigne, Biochemical Purification of a Mammalian Slit Protein as a Positive Regulator of Sensory Axon Elongation and Branching, Cell. 96 (1999) 771–784. doi:10.1016/S0092-8674(00)80588-7.

[36] G. Holmes, L. Niswander, Expression of slit-2 and slit-3 during chick development, Dev. Dyn. 222 (2001) 301–307. doi:10.1002/dvdy.1182.

[37] N. Vargesson, V. Luria, I. Messina, L. Erskine, E. Laufer, Expression patterns of Slit and Robo family members during vertebrate limb development, Mech. Dev. 106 (2001) 175–180. doi:10.1016/S0925-4773(01)00430-0.

[38] L. Camurri, E. Mambetisaeva, V. Sundaresan, Rig-1 a new member of Robo family genes exhibits distinct pattern of expression during mouse development, Gene Expr. Patterns. 4 (2004) 99–103. doi:10.1016/S1567-133X(03)00142-X.

[39] W.J. Zhou, Z.H. Geng, J.R. Spence, J.G. Geng, Induction of intestinal stem cells by R-spondin 1 and Slit2 augments chemoradioprotection, Nature. 501 (2013) 107–111. doi:10.1038/nature12416.

[40] H. Akiyama, J.P. Lyons, Y. Mori-Akiyama, X. Yang, R. Zhang, Z. Zhang, J.M. Deng, M.M. Taketo, T. Nakamura, R.R. Behringer, P.D. McCrea, B. De Crombrugghe, Interactions between Sox9 and β-catenin control chondrocyte differentiation, Genes Dev. 18 (2004) 1072–1087. doi:10.1101/gad.1171104.

[41] T. Komori, Regulation of osteoblast differentiation by transcription factors, J. Cell. Biochem. 99 (2006) 1233–1239. doi:10.1002/jcb.20958.

[42] M.A. El-Brolosy, D.Y.R. Stainier, Genetic compensation: A phenomenon in search of mechanisms., PLoS Genet. 13 (2017) e1006780. doi:10.1371/journal.pgen.1006780.

국문 요약

연구배경

본 연구자는 이전 연구에서 slit guidance ligand 3 (Slit3)가 골형성을 촉진하고 골흡수를 억제함을 보고한 바 있다. 이 연구를 진행 중 우연히 *Slit3*가 결핍된 마우스의 크기가 작은 것을 관찰하여, 본 연구에서는 Slit3가 장골의 길이 조절 기전이 연골내골화에 관여하는지 알아보고자 하였다.

연구내용 및 범위

1. *Slit3* 와 *Robo2* 결핍 마우스의 형태학적 분석
   - *Slit3* 결핍 마우스 장골의 형태학적 변화 관찰
   - *Slit3* 결핍 마우스 배아의 장골 변화 관찰
   - *Robo2* 결핍 마우스 배아의 장골 변화 관찰
2. Slit3의 세포학적 작용기전 연구
   - 연골세포에 Slit3를 처치 후 분화 확인
   - 연골 분화 표지자 확인
   - 연골세포에서 Wnt/β-catenin 신호 확인
   - Slit3 수용체 확인

연구방법 및 전략

- Slit3 knockout mouse; KO 마우스와 WT 비교 분석
- Robo2 knockout mouse; KO 마우스와 WT 비교 분석
- Histomorphology; H&E, alcian blue, von kossa와 IHC staining
- 연골 세포 실험; ATDC5 세포를 이용한 분화 및 증식 실험 및 연골 분화 마커확인, Slit3 수용체 확인
- 기전 연구; qRT-PCR, western blot, immunocytochemistry, luciferase

assay 등을 이용한 기전 연구

연구결과

배아 단계의 *Slit3* 결핍 마우스의 장골에서 골화가 지연되며, 연골의 비대화가 증가됨을 관찰하여, 연골세포 성숙이 지연됨을 시사하였다. Slit3 단백은 ATDC5 세포의 증식에는 영향 없이, COL1A1, SOX9, COL10A1, VEGF 및 MMP13 등의 분화 표지자의 발현을 촉진하였다. Slit3는 연골세포의 β-catenin 활성을 억제하였고, lithium chloride로 β-catenin 자극 시 Slit3에 의해 촉진되었던 연골 세포 분화를 방지할 수 있었다. Slit3의 수용체로 알려진 네 가지 Robo 형태 중, ATDC5 세포는 Robo2만 발현하였으며, *Robo2*를 siRNA로 억제 시 역시 Slit3에 의해 촉진되었던 연골 세포 분화를 방지할 수 있었다. 또한, *Robo2* 결핍 마우스에서도 장골의 골화가 지연되며, 연골의 비대화가 관찰되었다.

결론

Slit3/Robo2 시스템은 β-catenin 활성 억제를 통해 연골세포 성숙을 촉진하고 연골내골화를 유도할 것으로 판단되었다.

중심단어: Slit3, Robo2, Endochondral ossification, Chondrocytes, β-catenin